FULLY COMPUTABLE A POSTERIORI ERROR ESTIMATOR USING ANISOTROPIC FLUX EQUILIBRATION ON ANISOTROPIC MESHES*

NATALIA KOPTEVA†

Abstract. Fully computable a posteriori error estimates in the energy norm are given for singularly perturbed semilinear reaction-diffusion equations posed in polygonal domains. Linear finite elements are considered on anisotropic triangulations. To deal with the latter, we employ anisotropic quadrature and explicit anisotropic flux reconstruction. Prior to the flux equilibration, divergence-free corrections are introduced for pairs of anisotropic triangles sharing a short edge. We also give an upper bound for the resulting estimator, in which the error constants are independent of the diameters and the aspect ratios of mesh elements, and of the small perturbation parameter.

Key words. a posteriori error estimate, anisotropic triangulation, anisotropic flux equilibration, flux reconstruction, anisotropic quadrature, energy norm, singular perturbation, reaction-diffusion.

AMS subject classifications. 65N15, 65N30.

1. Introduction. We consider linear finite element approximations to singularly perturbed semilinear reaction-diffusion equations of the form

$$Lu := -\varepsilon^2 \triangle u + f(x,y;u) = 0 \quad \text{for } (x,y) \in \Omega, \qquad u = 0 \quad \text{on } \partial\Omega, \tag{1.1}$$

posed in a, possibly non-Lipschitz, polygonal domain $\Omega \subset \mathbb{R}^2$. Here $0 < \varepsilon \leqslant 1$. We also assume that f is continuous on $\Omega \times \mathbb{R}$ and satisfies $f(\cdot;s) \in L_\infty(\Omega)$ for all $s \in \mathbb{R}$, and the one-sided Lipschitz condition $f(x,y;u) - f(x,y;v) \geqslant C_f[u-v]$ whenever $u \geqslant v$, with some constant $C_f \geqslant 0$. Then there is a unique solution $u \in W^2_\ell(\Omega) \subseteq W^1_q \subset C(\bar\Omega)$ for some $\ell > 1$ and $q > 2$ [9, Lemma 1]. We additionally assume that $C_f + \varepsilon^2 \geqslant 1$ (as a division by $C_f + \varepsilon^2$ immediately reduces (1.1) to this case).

Our goal is to give explicitly and fully computable a posteriori error estimates on reasonably general anisotropic meshes (such as on Fig. 2.1 and Fig. 2.2) in the energy norm defined by

$$|\!|\!| v |\!|\!|_{\varepsilon;\Omega} := \left\{ \varepsilon^2 \|\nabla v\|^2_{2;\Omega} + C_f \|v\|^2_{2;\Omega} \right\}^{1/2}.$$

This goal is achieved by a certain combination of explicit flux reconstruction and flux equilibration.

Flux equilibration for equations of type (1.1) was considered in [1, 3, 4, 7] on shape-regular meshes (see also [2, Chap. 6] for the case $\varepsilon = 1$), and in [10] on anisotropic meshes. The estimators in [3, 4, 7] are based on flux reconstructions, while [1, 10] employ solutions of certain local problems.

Our approach in this paper differs from the previous work in a few ways.

- The fluxes are equilibrated within a local patch using anisotropic weights depending on the local, possibly anisotropic, mesh geometry (see (5.3)).
- Prior to the flux equilibration, divergence-free corrections are introduced for pairs of anisotropic triangles sharing a short edge (see §6, in particular, (6.2)).
- A certain anisotropic quadrature is used on anisotropic elements (see §3). This is motivated by some observations made in [13], and also enables us to drop some mesh assumptions made in recent papers [14, 15].

*The author was partially supported by Science Foundation Ireland grant SFI/12/IA/1683

†Department of Mathematics and Statistics, University of Limerick, Limerick, Ireland (natalia.kopteva@ul.ie).

- Our estimator is explicitly and fully computable in the sense that it involves no unknown error constants (unlike other estimators on anisotropic meshes, such as in [10, 14, 15]).
- In contrast to [10], an upper bound for our estimator involves no matching functions (which we discuss below). In fact, the error constant C in the upper bound (1.2) is independent not only of the diameters and the aspect ratios of mesh elements, but also of the small perturbation parameter ε.

The robustness of our estimator, denoted by $\mathcal{E}$, with respect to the mesh aspect ratios, as well as the small perturbation parameter ε, is demonstrated by the following upper bound (which follows from Theorems 4.1 and 4.3):

$$\mathcal{E} \lesssim C \Big\{ \sum_{z\in\mathcal{N}} \big\| \min\{1,\, \varepsilon H_T h_T^{-2}\}^{1/2}\, \varepsilon J_z \big\|_{\omega_z}^2 + \sum_{z\in\mathcal{N}} \big\| \min\{1,\, h_z\varepsilon^{-1}\}\, f_h^I \big\|_{\omega_z}^2 + \big\| f_h - f_h^I \big\|_\Omega^2 + \sum_{T\in\mathcal{T}} \big\| \lambda_T \operatorname{osc}(f_h^I; T) \big\|_T^2 + \sum_{z\in\mathcal{N}_{\partial\Omega}^*} \big\| \lambda_T f_h(z) \big\|_{\omega_z}^2 \Big\}^{1/2}, \tag{1.2}$$

where C is independent of the diameters and the aspect ratios of elements in the triangulation $\mathcal{T}$, and of ε. Here $\mathcal{N}$ is the set of nodes in $\mathcal{T}$, and ω_z is the patch of elements surrounding any $z \in \mathcal{N}$, while J_z is the maximum within ω_z of the standard jump in the normal derivative of the computed solution u_h across an element edge, $f_h = f(\cdot; u_h)$ and f_h^I is its standard piecewise-linear Lagrange interpolant. We also use $\lambda_T = \min\{1,\, H_T\varepsilon^{-1}\}$, $H_T \simeq \operatorname{diam}(T)$, $h_T \simeq H_T^{-1}|T|$, and $h_z \simeq |\omega_z|/\operatorname{diam}(\omega_z)$. The boundary subset $\mathcal{N}_{\partial\Omega}^*$ of $\mathcal{N}$ is defined by (2.4).

To relate (1.2) to interpolation error bounds (as well as to possible adaptive-mesh construction strategies), note that $|J_z|$ may be interpreted as approximating the diameter of ω_z under the metric induced by the squared Hessian matrix of the exact solution (while f_h^I approximates $\varepsilon^2 \triangle u$). Note also that the right-hand side in (1.2) is similar to the estimator in the recent paper [15], and reduces, in the case of shape-regular meshes, to a version of the estimator given by [23].

Explicit residual-type a posteriori error estimates for problems of type (1.1) were also given in [23, 9] on shape-regular meshes, [22, 12, 6] on anisotropic tensor-product meshes, and [18, 20, 19, 14, 15, 16] on more general anisotropic meshes (for $\varepsilon = 1$ in [22, 18]). All these estimates are not fully guaranteed in the sense that they involve unknown error constants. (The cited papers deal with the energy norm, except for [6, 9, 12, 14] addressing the maximum norm.)

Note that the error constants in the estimators of [18, 19, 20] (as well as the upper bound for the estimator [10] that we already mentioned) involve the so-called matching functions. The latter depend on the unknown error and take moderate values only when the grid is either isotropic, or, being anisotropic, is aligned correctly to the solution, while, in general, they may be as large as mesh aspect ratios. The presence of such matching functions in the estimator is clearly undesirable, and is entirely avoided in recent papers [14, 15, 16], as well as in our upper bound (1.2).

Finally, note that a posteriori error estimation on anisotropic meshes presents a more serious challenge not only compared to the shape-regular-mesh case, but also to the a priori error estimation. Indeed, there is a vast number of papers showing that a-priori-chosen anisotropic meshes offer an efficient way of computing reliable numerical approximations of solutions that exhibit sharp boundary and interior layers. In the context of singularly perturbed differential equations, such as (1.1) with $\varepsilon \ll 1$, see, for example, [8, 11, 17, 21] and references therein.

The paper is organized as follows. In §2, we list all triangulation assumptions. Next, §3 describes the considered finite element discretization with quadrature. The structure of the reconstructed flux and the main results are presented in §4. The case $h_z \lesssim \varepsilon$ is addressed in §§5–6, while §7 deals with the case $h_z \gtrsim \varepsilon$. We conclude the paper by presenting some numerical results in §8.

Notation. We write $a \simeq b$ when $a \lesssim b$ and $a \gtrsim b$, $a = \mathcal{O}(b)$ when $|a| \lesssim b$, and $a \lesssim b$ when $a \leqslant Cb$ with a generic constant C depending on Ω and f, but C does not depend on either ε or the diameters and the aspect ratios of elements in $\mathcal{T}$. Also, we write $a \ll b$ when $a < c_0 b$ with a fixed small constant c_0 (used to distinguish between anisotropic and isotropic elements). The indicator function $\mathbb{1}_A$ takes value 1 if condition A is satisfied, and vanishes otherwise. For any $\mathcal{D} \subset \Omega$, we let $\|\cdot\|_{\mathcal{D}} = \|\cdot\|_{L_2(\mathcal{D})}$, while $\boldsymbol{\nu}$ and $\boldsymbol{\mu}$, possibly subscripted, denote the unit vectors on $\partial\mathcal{D}$ in the outward normal and counterclockwise tangential direction, respectively. For any triangles T and T' sharing an edge, a standard notation is used:

$$\big[\boldsymbol{\tau}\cdot\boldsymbol{\nu}\big]_{\partial T\cap\partial T'} := \boldsymbol{\tau}\cdot\boldsymbol{\nu}\big|_T + \boldsymbol{\tau}\cdot\boldsymbol{\nu}\big|_{T'}\,, \qquad \big[\partial_{\boldsymbol{\nu}} u_h\big]_{\partial T\cap\partial T'} := \big[\nabla u_h\cdot\boldsymbol{\nu}\big]_{\partial T\cap\partial T'}\,.$$

2. Triangulation assumptions. We shall use z, S and T to respectively denote particular mesh nodes, edges and elements, while $\mathcal{N}$, $\mathcal{S}$ and $\mathcal{T}$ will respectively denote their sets. For each $T \in \mathcal{T}$, let H_T be the maximum edge length and $h_T := 2H_T^{-1}|T|$ be the minimum height in T. For each $z \in \mathcal{N}$, let ω_z be the patch of elements surrounding any $z \in \mathcal{N}$, $\mathcal{S}_z$ the set of edges originating at z, and

$$H_z := \operatorname{diam}(\omega_z), \quad h_z := \max_{T\subset\omega_z} h_T, \quad \mathring{h}_z := \min_{T\subset\omega_z} h_T, \quad \gamma_z := \mathcal{S}_z\backslash\partial\Omega. \tag{2.1}$$

We shall also employ the standard basis hat functions $\{\phi_z\}_{z\in\mathcal{N}}$.

Throughout the paper we make some triangulation assumptions. All of them are automatically satisfied by shape-regular triangulations.

- *Maximum Angle condition.* Let the maximum interior angle in any triangle $T \in \mathcal{T}$ be uniformly bounded by some positive $\lambda_0 < \pi$.
- Let the number of triangles containing any node be uniformly bounded.
- For any $z \in \mathcal{N}$, one has

$$h_T \simeq \mathring{h}_z \ \text{ and } \ H_T \simeq H_z \qquad \text{or} \qquad h_T \simeq H_T \qquad \forall\ T \subset \omega_z. \tag{2.2}$$

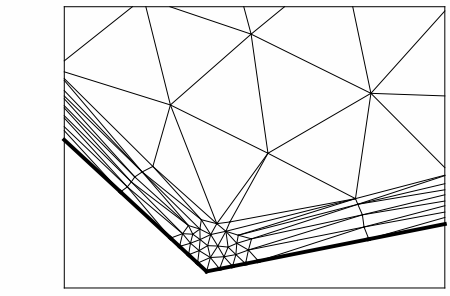

FIG. 2.1. *Example of a mesh that satisfies all assumptions made in §2 (including $\mathcal{A}1$ and $\mathcal{A}2$).*

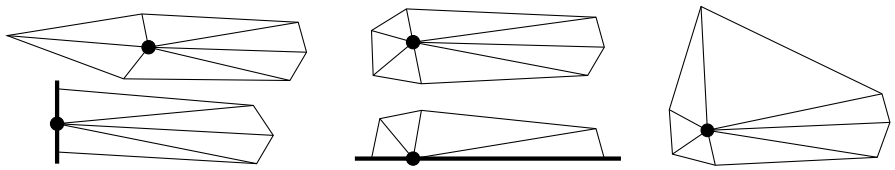

FIG. 2.2. *Examples of anisotropic nodes $z \in \mathcal{N}_{\rm ani}$ (left), nodes $z \in \mathcal{N}\backslash(\mathcal{N}_{\rm ani} \cup \mathcal{N}_{\rm iso})$ (centre), an isotropic node $z \in \mathcal{N}_{\rm iso}$ (right), and a node $z \in \mathcal{N}^*_{\partial\Omega}$ (bottom left). Examples of nodes that satisfy $\mathcal{A}1^*_{\rm ani}$ (top left), $\mathcal{A}1_{\rm ani}$ (bottom left), and $\mathcal{A}1_{\rm mix}$ (centre and right).*

We also distinguish subsets $\mathcal{N}_{\rm ani}$, $\mathcal{N}_{\rm iso}$ and $\mathcal{N}^*_{\partial\Omega}$ of $\mathcal{N}$ (see Fig. 2.2). Note that $\mathcal{N}_{\rm ani} \cap \mathcal{N}_{\rm iso} = \varnothing$, while $\mathcal{N}\backslash(\mathcal{N}_{\rm ani} \cup \mathcal{N}_{\rm iso})$ is not necessarily empty.

(1) *Anisotropic nodes*, whose set is denoted by $\mathcal{N}_{\rm ani}$, are such that

$$h_z \ll H_z, \qquad h_T \simeq h_z \ \text{ and } \ H_T \simeq H_z \quad \forall\ T \subset \omega_z. \tag{2.3}$$

Note that (2.3) implies (2.2), while $z \in \mathcal{N}_{\rm ani}$ implies $\mathring{h}_z \simeq h_z$.

(2) *Isotropic nodes*, to whose set we shall refer as $\mathcal{N}_{\rm iso}$, are such that $h_z \simeq H_z$.

(3) One may expect anisotropic elements near the boundary to be aligned along it. To distinguish some boundary nodes for which it is not the case, we introduce

$$\mathcal{N}^*_{\partial\Omega} := \big\{z \in \mathcal{N}_{\rm ani} \cap \partial\Omega\backslash\{\text{corners of } \Omega\} \text{ and } |\mathcal{S}_z \cap \partial\Omega| \simeq h_z \lesssim \varepsilon\big\}. \tag{2.4}$$

Occasionally, we shall make additional assumptions that we describe below.

$\mathcal{A}1$ Each $z \in \mathcal{N}$ with $h_z \lesssim \varepsilon$ satisfies $z \in \mathcal{N}_{\rm ani}\backslash\{\text{corners of } \Omega\}$ and condition $\mathcal{A}1_{\rm ani}$, or it satisfies condition $\mathcal{A}1_{\rm mix}$; see below.

$\mathcal{A}1_{\rm ani}$ *Quasi-non-obtuse anisotropic elements.* Let the maximum triangle angle at $z \in \mathcal{N}_{\rm ani}$ be bounded by $\frac{\pi}{2} + \lambda_1 \frac{h_z}{H_z}$ for some positive constant λ_1.

$\mathcal{A}1_{\rm mix}$ With $\mathring{\mathcal{S}}_z := \{S \subset \mathcal{S}_z : |S| \simeq \mathring{h}_z\}$ and $\mathring{\omega}_z := \{T \subset \omega_z : h_T \simeq H_T \simeq \mathring{h}_z\}$ respectively denoting the sets of edges and isotropic triangles of diameter $\simeq \mathring{h}_z$ within ω_z, let $(\mathring{\omega}_z \cup \mathring{\mathcal{S}}_z)\backslash\{z\}$ be connected.

$\mathcal{A}2$ Each $z \in \mathcal{N}$ with $h_z \gtrsim \varepsilon$ satisfies $\mathring{h}_z \geqslant \sqrt{6}\varepsilon$.

Note that $\mathcal{A}1_{\rm ani}$ is always satisfied by isotropic elements, so it requires only some of the anisotropic part of the mesh to be close to a non-obtuse triangulation. $\mathcal{A}1_{\rm mix}$ is also always satisfied on shape-regular meshes (as then $\mathring{\omega}_z = \omega_z$). For anisotropic nodes, $\mathcal{A}1_{\rm mix}$ may be satisfied if $z \in \partial\Omega$ (in this case, $\mathring{\omega}_z = \varnothing$, while $\mathring{\mathcal{S}}_z\backslash\{z\}$ is connected only if $\mathring{\mathcal{S}}$ contains a single edge). Note also that $\mathcal{A}2$ is satisfied for any $z \notin \mathcal{N}_{\rm iso}$, while for isotropic nodes it does impose a mild restriction (as for the latter, $h_z \simeq H_z$, so whenever $H_z \gtrsim \varepsilon$, within ω_z we impose $h_T \geqslant \sqrt{6}\varepsilon$).

We shall also consider a weaker version of $\mathcal{A}1$.

$\mathcal{A}1^*$ Each $z \in \mathcal{N}$ with $h_z \lesssim \varepsilon$ satisfies $z \in \mathcal{N}_{\rm ani}\backslash\partial\Omega$ and condition $\mathcal{A}1^*_{\rm ani}$, or $z \in \mathcal{N}^*_{\partial\Omega}$ and satisfies $\mathcal{A}1_{\rm ani}$, or it satisfies condition $\mathcal{A}1_{\rm mix}$.

$\mathcal{A}1^*_{\rm ani}$ *Local Element Orientation condition.* For $z \in \mathcal{N}_{\rm ani}$, there exists a rectangle $R_z \supset \omega_z$ such that $|R_z| \simeq |\omega_z|$.

3. Finite element method with quadrature. We discretize (1.1) using linear finite elements. Let $S_h \subset H^1_0(\Omega) \cap C(\bar\Omega)$ be a piecewise-linear finite element space relative to a triangulation $\mathcal{T}$, and let the computed solution $u_h \in S_h$ satisfy

$$\varepsilon^2\langle\nabla u_h, \nabla v_h\rangle + \langle f_h, v_h\rangle_h = 0 \quad \forall\ v_h \in S_h, \qquad f_h(\cdot) := f(\cdot; u_h). \tag{3.1}$$

Here $\langle\cdot,\cdot\rangle$ is the $L_2(\Omega)$ inner product, and $\langle\cdot,\cdot\rangle_h$ is its quadrature approximation.

We now describe $\langle f_h, v_h\rangle_h$ used in (3.1). For the integral over $T \in \mathcal{T}$, a quadrature formula Q_T is employed, which is anisotropic on a certain subset $\mathcal{T}^*$ of anisotropic elements:

$$Q_T(w) = |T| \sum_{j=1}^{3} \theta_{T;z_j} w(z_j) := \begin{cases} \frac{1}{3}|T|\big(w(z_1) + w(z_2) + w(z_3)\big) & \text{for } T \in \mathcal{T}\backslash\mathcal{T}^*, \\ \frac{1}{2}|T|\big(w(z_1) + w(z_2)\big) & \text{for } T \in \mathcal{T}^*. \end{cases} \tag{3.2}$$

Here $\{z_j\}_{j=1}^3$ are the vertices of T, with $z_3 =: z^*$ opposite the shortest edge, while

$$\mathcal{T}^* := \{T \in \mathcal{T} : h_T \ll H_T \text{ and } h_T \lesssim \varepsilon\} \setminus \mathcal{T}_0\,, \tag{3.3}$$

with $\mathcal{T}_0 \subset \{T \in \mathcal{T} : z^* \in \mathcal{N}_{\rm iso} \text{ and } z_1, z_2 \notin \mathcal{N}_{\rm ani}\backslash\partial\Omega\}$ (so, unless one wants to minimize $\mathcal{T}^*$, the simplest option is $\mathcal{T}_0 := \varnothing$). Now, let

$$\langle f_h, v_h\rangle_h := \sum_{T\in\mathcal{T}\backslash\mathcal{T}^*} Q_T(f_h v_h) + \sum_{T\in\mathcal{T}^*} Q_T(\bar f_h v_h), \tag{3.4}$$

where

$$\bar f_h = \bar f_{h;T} := \tfrac{1}{3}[f_h(z_1) + f_h(z_2) + f_h(z_3)] \quad \forall\ T \in \mathcal{T}. \tag{3.5}$$

As $\bar f_h$ is an elementwise constant approximation of f_h, so $Q_T(\bar f_h v_h) = \bar f_{h,T} Q_T(v_h)$.

Note that the discretization (3.1), (3.2), (3.3), (3.4) can be written as

$$\sum_{S\subset\gamma_z} \tfrac{1}{2}\varepsilon^2|S|\big[\partial_{\boldsymbol\nu} u_h\big]_S + \sum_{T\subset\omega_z} \theta_{T;z}|T|\, F_{T;z} = 0 \qquad \forall\ z \in \mathcal{N}\backslash\partial\Omega, \tag{3.6}$$

where $F_{T;z} := f_h(z)$ for $T \in \mathcal{T}\backslash\mathcal{T}^*$ and $F_{T;z} := \bar f_{h;T}$ for $T \in \mathcal{T}^*$. It will be sometimes convenient to replace the second sum here using an average $\bar F_z$ of $F_{T;z}$, associated with z, defined by

$$\bar F_z \sum_{T\subset\omega_z} \theta_{T;z}|T| := \sum_{T\subset\omega_z} \theta_{T;z}|T|\, F_{T;z} \quad \forall\ z \notin \partial\Omega, \qquad \bar F_z := f_h(z) \quad \forall\ z \in \partial\Omega. \tag{3.7}$$

Remark 3.1. The above quadrature yields the standard linear lumped-mass finite element discretization on $\mathcal{T}\backslash\mathcal{T}^*$. On $\mathcal{T}^*$, a special anisotropic quadrature is employed (designed to address certain convergence issues reported in [13]). The resulting method may be also interpreted as the vertex-centered finite volume method (or the box method) with a special choice of control volumes, applied to the approximation of our equation $-\varepsilon^2\triangle u + \overline{f(\cdot;u)} = 0$. A related interpretation as a Petrov-Galerkin method is also possible.

Remark 3.2. Our results remain valid, if $Q_T(f_h v_h)$ is replaced by $Q_T(\bar f_h v_h)$ in the first sum in (3.4)*. However, using $Q_T(f_h v_h)$ for $h_T \gg \varepsilon$ yields a superior discretization (as in this case the local stiffness matrices become negligible so diagonal mass matrices are preferable). On the other hand, replacing $Q_T(\bar f_h v_h)$ by $Q_T(f_h v_h)$ in the second sum in* (3.4) *yields a less standard lumped-mass discretization on $\mathcal{T}^*$. For the latter choice, our estimator will enjoy a version of the upper bound* (1.2) *with λ_T replaced by 1 whenever $h_T \ll H_T \lesssim \varepsilon$. Furthermore, all our results remain valid without any changes if $Q_T(\bar f_h v_h)$ is used only for $T \in \mathcal{T}^* : H_T \lesssim \varepsilon$.*

4. A posteriori error estimator. Main Results. We start with a relatively standard auxiliary result, a version of which can be found, for example, in [3, Lemma 1] and [7, Theorem 3.1].

THEOREM 4.1. *For any $u_h \in S_h$, let $\boldsymbol{\tau} \in H^1(\mathrm{div}, T)$ $\forall T \in \mathcal{T}$ also satisfy*

$$[\boldsymbol{\tau} \cdot \boldsymbol{\nu}] = [\partial_{\boldsymbol{\nu}} u_h] \qquad \text{on all } S \in \mathcal{S} \backslash \partial\Omega. \tag{4.1}$$

Then, for a solution u of (1.1), with $C_f > 0$, one has

$$|||u_h - u|||_{\varepsilon;\Omega} \leqslant \mathcal{E} := \left\{ \|\varepsilon \boldsymbol{\tau}\|_\Omega^2 + C_f^{-1} \|\varepsilon^2 \mathrm{div}\boldsymbol{\tau} + f_h\|_\Omega^2 \right\}^{1/2}. \tag{4.2}$$

Proof. With $v := u_h - u$, one has

$$\begin{aligned} |||u_h - u|||_{\varepsilon;\Omega}^2 &\lesssim \varepsilon^2 \langle \nabla(u_h - u), \nabla v\rangle + \langle f(\cdot; u_h) - f(\cdot; u), v\rangle \\ &= \varepsilon^2 \langle \nabla u_h, \nabla v\rangle + \langle f(\cdot; u_h), v\rangle, \\ &= \varepsilon^2 \langle \boldsymbol{\tau}, \nabla v\rangle + \langle \varepsilon^2 \mathrm{div}\boldsymbol{\tau} + f_h, v\rangle, \end{aligned}$$

which immediately implies (4.2). Here we employed the observation (obtained using $\triangle u_h = 0$ in any T, and (4.1)) that

$$\langle \nabla u_h, \nabla v\rangle + \langle \underbrace{\triangle u_h}_{=0}, v\rangle = \sum_{S \in \mathcal{S}} \int_S v \underbrace{[\partial_{\boldsymbol{\nu}} u_h]}_{=[\boldsymbol{\tau}\cdot\boldsymbol{\nu}]} = \langle \boldsymbol{\tau}, \nabla v\rangle + \langle \mathrm{div}\boldsymbol{\tau}, v\rangle.$$

Note that here (as well as in (4.2)), with slight abuse of notation, we understood $\triangle u_h$ and $\mathrm{div}\boldsymbol{\tau}$ as regular functions in Ω defined elementwise. □

*Remark 4.2 (*Cases $C_f \geqslant 0$ and $C_f = C_f(x, y)$*). An inspection of the above proof shows that the estimator $\mathcal{E}$ in (4.2) can be replaced by a more general*

$$\mathcal{E} := \left\{ (1-\vartheta)^{-1} \|\varepsilon \boldsymbol{\tau}\|_\Omega^2 + \left(C_f + \varepsilon^2 C_\Omega^{-2} \vartheta\right)^{-1} \|\varepsilon^2 \mathrm{div}\boldsymbol{\tau} + f_h\|_\Omega^2 \right\}^{1/2},$$

where C_Ω is the Poincaré constant, and $\vartheta \in [0, 1)$ is an arbitrary constant, with $\vartheta > 0$ unless $C_f > 0$. Note also that if $C_f = C_f(x, y)$, the above result remains valid with an obvious modification of the energy norm to $|||v|||_{\varepsilon;\Omega} := \left\{ \varepsilon^2 \|\nabla v\|_\Omega^2 + \|C_f^{1/2} v\|_\Omega^2 \right\}^{1/2}$ and a similar modification of $\mathcal{E}$.

4.1. Structure of $\boldsymbol{\tau}$. Clearly, $\boldsymbol{\tau}$ that satisfies the conditions of Theorem 4.1 is not unique, and there are various choice available in the literature.

Our task in this paper is to explicitly define $\boldsymbol{\tau}$ to be used in (4.2) in a way that is appropriate for anisotropic meshes. We introduce a suitable $\boldsymbol{\tau}$ in the form

$$\boldsymbol{\tau} := \sum_{z \in \mathcal{N}} \boldsymbol{\tau}_z + \sum_{T \in \mathcal{T}^f} \boldsymbol{\tau}_T^f + \sum_{S \in \mathcal{S}^*} \boldsymbol{\tau}_S^J, \qquad \mathcal{T}^f := \{T \in \mathcal{T} : H_T \lesssim \varepsilon\}, \tag{4.3}$$

where $\boldsymbol{\tau}_z$, $\boldsymbol{\tau}_T^f$, and $\boldsymbol{\tau}_S^J$ have support on ω_z, T, and $T \cup T'$ for $S = \partial T \cap \partial T'$, respectively. It is also convenient to set $\boldsymbol{\tau}_T^f$ and $\boldsymbol{\tau}_S^J$ to 0 whenever respectively $T \notin \mathcal{T}^f$ and $S \notin \mathcal{S}^*$. Under condition $\mathcal{A}1$, we set $\mathcal{S}^* := \varnothing$, while otherwise $\mathcal{S}^*$ is essentially the set of short edges shared by pairs of anisotropic triangles (see §6 for details).

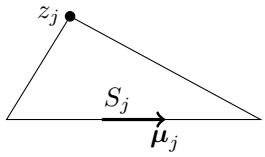

FIG. 4.1. *Notation used in* (4.6)*: the edge S_j is opposite to the vertex z_j, the counterclockwise tangential unit vector $\boldsymbol{\mu}_j$ lies along S_j.*

To be more precise, in the case $\mathcal{S}^* = \varnothing$, the function $\boldsymbol{\tau}_z$, with support on ω_z, is simply required to satisfy

$$[\boldsymbol{\tau}_z \cdot \nu] = \phi_z[\partial_{\boldsymbol{\nu}} u_h] \text{ on } \gamma_z, \qquad \boldsymbol{\tau}_z \cdot \nu = 0 \text{ on } \partial\omega_z \backslash \partial\Omega. \tag{4.4}$$

The function $\boldsymbol{\tau}_T$, with support in T, satisfies

$$\boldsymbol{\tau}_T \cdot \nu = 0 \quad \text{on } \partial T \quad \text{and} \quad \varepsilon^2 \mathrm{div} \boldsymbol{\tau}_T + (f_h^I - \bar{f}_h) = 0 \quad \text{in } T \qquad \forall\, T \in \mathcal{T}^f, \tag{4.5}$$

and is explicitly defined (see, e.g., [3, (22)]) by

$$\boldsymbol{\tau}_T^f := \gamma_1\phi_2\phi_3|S_1|\boldsymbol{\mu}_1 + \gamma_2\phi_3\phi_1|S_2|\boldsymbol{\mu}_2 + \gamma_3\phi_1\phi_2|S_3|\boldsymbol{\mu}_3, \qquad \gamma_j := \tfrac{1}{3}\varepsilon^{-2}\nabla f_h^I \cdot |S_j|\boldsymbol{\mu}_j\,, \tag{4.6}$$

where $\{z_j\}_{j=1}^3$ are the vertices of T with the corresponding basis functions $\phi_j := \phi_{z_j}$, and for $j = 1, 2, 3$, the edge S_j is opposite to z_j, while the counterclockwise tangential unit vector $\boldsymbol{\mu}_j$ lies along S_j; see Fig. 4.1.

4.2. Upper bound for the estimator. In this section, we present a theorem, which, combined with (4.2), gives the upper bound (1.2) for the estimator $\mathcal{E}$. At the same time, this theorem provides valuable information on the local properties of the components of $\boldsymbol{\tau}$ in (4.3). These components (except for $\boldsymbol{\tau}_T^f$) are constructed and analyzed in §§5–6 for the case $h_z \lesssim \varepsilon$, and in §7 for the case $h_z \gtrsim \varepsilon$. So, with the exception of (4.9), all bounds in the following theorem will be obtained in these forthcoming sections. (To be more precise, here we summarize the results of Lemmas 5.3, 5.4, 6.3 and 7.3.)

THEOREM 4.3. *Let u_h solve* (3.1) *with $\langle\cdot,\cdot\rangle_h$ defined in §3, and set*

$$J_z := \max_{S\subset\gamma_z} \Big|[\partial_{\boldsymbol{\nu}} u_h]_S\Big|, \qquad \lambda_T := \min\{1,\, H_T\varepsilon^{-1}\} \text{ and } \lambda'_T := \min\{1,\, \varepsilon H_T h_T^{-2}\} \ \forall T \in \mathcal{T}.$$

(i) Under conditions $\mathcal{A}1$ and $\mathcal{A}2$, one can construct $\boldsymbol{\tau}$, subject to (4.1)*, in the form* (4.3) *with $\mathcal{S}^* = \varnothing$, where $\boldsymbol{\tau}_z$ and an associated function g_z, both with support in ω_z, satisfy, for any $z \in \mathcal{N}$,*

$$\sum_{\substack{z\in\mathcal{N}:\\ h_z\lesssim\varepsilon}} \varepsilon^2 \mathrm{div}\boldsymbol{\tau}_z + \bar{f}_h = \sum_{z\in\mathcal{N}} g_z \quad \text{in } \Omega, \tag{4.7}$$

$$\mathbb{1}_{h_z\gtrsim\varepsilon}\, \|\varepsilon^2 \mathrm{div}\boldsymbol{\tau}_z\|_{\omega_z} + \|\varepsilon\boldsymbol{\tau}_z\|_{\omega_z} + \|g_z\|_{\omega_z} \lesssim \|\lambda_T'^{1/2}\varepsilon J_z\|_{\omega_z} + \min\{1,\, h_z\varepsilon^{-1}\}\|f_h^I\|_{\omega_z} + \sum_{T\subset\omega_z} \lambda_T \|\mathrm{osc}(f_h^I; T)\|_T + \mathbb{1}_{z\in\mathcal{N}_{\partial\Omega}^*}\, \|\lambda_T f_h(z)\|_{\omega_z}, \tag{4.8}$$

while $\boldsymbol{\tau}_T^f$ from (4.6) *satisfies* (4.5)*, and, for any $T \in \mathcal{T}$,*

$$\|\varepsilon^2 \mathrm{div}\boldsymbol{\tau}_T^f + (f_h - \bar{f}_h)\|_T + \|\varepsilon\boldsymbol{\tau}_T^f\|_T \lesssim \lambda_T \|\mathrm{osc}(f_h^I; T)\|_T + \|f_h - f_h^I\|_T. \tag{4.9}$$

(ii) Under conditions $\mathcal{A}1^*$ and $\mathcal{A}2$, one can construct $\boldsymbol{\tau}$, subject to (4.1)*, in the form* (4.3) *with $\mathcal{S}^* \neq \varnothing$, such that the above relations* (4.7), (4.8), (4.9) *hold true and, in addition, for any $S = \partial T \cap \partial T' \in \mathcal{S}^*$,*

$$\mathrm{div}\boldsymbol{\tau}_S^J = 0 \ \text{ in } T \cup T', \qquad \left\|\varepsilon\boldsymbol{\tau}_S^J\right\|_{T\cup T'} \lesssim \left\|\varepsilon[\partial_{\boldsymbol{\nu}} u_h]_S\right\|_{T\cup T'}, \qquad \lambda'_T \simeq 1. \tag{4.10}$$

Proof of (4.9). If $T \in \mathcal{T}^f$, so, by (4.3), $\lambda_T \simeq H_T\varepsilon^{-1}$, a calculation [3, §3.3] shows that (4.6) implies (4.5), while $|\gamma_j| \lesssim \varepsilon^{-2}\mathrm{osc}(f_h^I;T)$ yields $|\varepsilon\boldsymbol{\tau}_T^f| \lesssim H_T\varepsilon^{-1}\mathrm{osc}(f_h^I;T)$. The desired bound (4.9) for $T \in \mathcal{T}^f$ follows. Otherwise, i.e. if $T \notin \mathcal{T}^f$, so $\lambda_T \simeq 1$, one has $\boldsymbol{\tau}_T^f = 0$, while $|f_h - \bar{f}_h| \leqslant |f_h - f_h^I| + \mathrm{osc}(f_h^I;T)$, so we again get (4.9). □

Remark 4.4. Note that for $z \in \mathcal{N}_{\partial\Omega}^*$, the bound (4.8) *involves $\lambda_T|f_h(z)| \simeq \min\{\varepsilon^{-1}, H_z^{-1}\}\, H_z|f_h(z)|$, where $\varepsilon^{-2}H_z|f_h(z)|$ may be interpreted as the diameter of ω_z under the metric induced by the squared Hessian matrix of the exact solution at $z \in \partial\Omega$. Indeed, as $u = 0$ on $\partial\Omega$, the Hessian matrix involves only the normal derivatives, while $\varepsilon^{-2}f_h = \varepsilon^{-2}f(\cdot;0) = \partial_{\boldsymbol{\nu}}^2 u$ on $\partial\Omega$; see also the definition of $\mathcal{N}_{\partial\Omega}^*$.*

5. Construction of $\boldsymbol{\tau}_z$ for $h_z \lesssim \varepsilon$ under condition $\mathcal{A}1$. Let the patch ω_z be formed by N_z triangles $\{T_i\}_{i=1}^{N_z} \subset \mathcal{T}$, numbered counterclockwise so that γ_z is formed by the edges $\partial T_{i-1} \cap \partial T_i$ for $i = 1, \dots, N_z$ if $z \notin \partial\Omega$ (with the notation $T_0 := T_{N_z}$), and for $i = 2, \dots, N_z$ if $z \in \partial\Omega$ (see Fig. 5.1 (left, centre)). For each $T_i \subset \omega_z$, let z be opposite to the edge denoted S_i, with the outward normal and the counterclockwise tangential unit vectors denoted $\boldsymbol{\nu}_i$ and $\boldsymbol{\mu}_i$ (see Fig. 5.1 (right)).

Define $\boldsymbol{\tau}_z$ associated with z by

$$\boldsymbol{\tau}_z := \phi_z\big(\alpha_i\boldsymbol{\nu}_i + \beta_i d_i^{-1}\boldsymbol{\mu}_i\big), \quad \alpha_i := \varepsilon^{-2}d_i\theta_{T_i;z}\widetilde{F}_{T_i;z}, \quad d_i := 2|T_i|\,|S_i|^{-1}, \tag{5.1a}$$

$\forall\ T_i \subset \omega_z$, where, using $F_{T;z}$ and $\bar{F}_z$ from (3.6), (3.7),

$$\widetilde{F}_{T;z} := \begin{cases} \bar{F}_z & \text{if } H_z \gtrsim \varepsilon \text{ and } z \in \mathcal{N}_{\mathrm{ani}}, \\ F_{T;z} & \text{otherwise.} \end{cases} \tag{5.1b}$$

Here we require $\{\beta_i\}_{i=1}^{N_z}$ to satisfy

$$\beta_{i-1} - \beta_i + \alpha_{i-1}\boldsymbol{\nu}_{i-1}\cdot|S_{i-1}^+|\boldsymbol{\nu}_{i-1}^+ + \alpha_i\boldsymbol{\nu}_i\cdot|S_i^-|\boldsymbol{\nu}_i^- = |S_i^-|\big[\partial_{\boldsymbol{\nu}}u_h\big]_{\partial T_{i-1}\cap\partial T_i} \tag{5.1c}$$

for $i = 1, \dots, N_z$ if $z \notin \partial\Omega$, and for $i = 2, \dots, N_z$ if $z \in \partial\Omega$. We use the notation $S_i^\pm := \partial T_i \cap \partial T_{i\pm1}$, as well as $\boldsymbol{\nu}_i^\pm$ and $\boldsymbol{\mu}_i^\pm$ for the outward normal and the counterclockwise tangential unit vectors of the edge $S_i^\pm$ in triangle T_i (see Fig. 5.1 (right)).

LEMMA 5.1. *Let $h_z \lesssim \varepsilon$. Then relations* (5.1) *for $\boldsymbol{\tau}_z$ imply* (4.4) *and*

$$\varepsilon^2\mathrm{div}\boldsymbol{\tau}_z + \theta_{T;z}\widetilde{F}_{T;z} = 0 \qquad \forall\ T \subset \omega_z, \tag{5.2a}$$

$$\|\varepsilon\boldsymbol{\tau}_z\|_{\omega_z} \lesssim \|h_z\varepsilon^{-1}f_h^I\|_{\omega_z} + \varepsilon\Big\{\sum_{i=1}^{N_z}\beta_i^2 d_i^{-2}|T_i|\Big\}^{1/2}. \tag{5.2b}$$

The system (5.1c) *for $\{\beta_i\}_{i=1}^{N_z}$ is consistent and has infinitely many solutions.*

Proof. Combining $\mathrm{div}(\phi_z\boldsymbol{\mu}_i) = \nabla\phi_z\cdot\boldsymbol{\mu}_i = 0$ with $\mathrm{div}(\phi_z\boldsymbol{\nu}_i) = \nabla\phi_z\cdot\boldsymbol{\nu}_i = -d_i^{-1}$ one gets $\mathrm{div}\boldsymbol{\tau}_z + \alpha_i d_i^{-1} = 0$ in $T_i \subset \omega_z$, which immediately implies (5.2a). For (5.2b), note that $d_i\theta_{T_i;z} \lesssim h_z\theta_{T_i;z}$, because, in view of (3.2), (3.3), unless $d_i \lesssim h_z$, one has

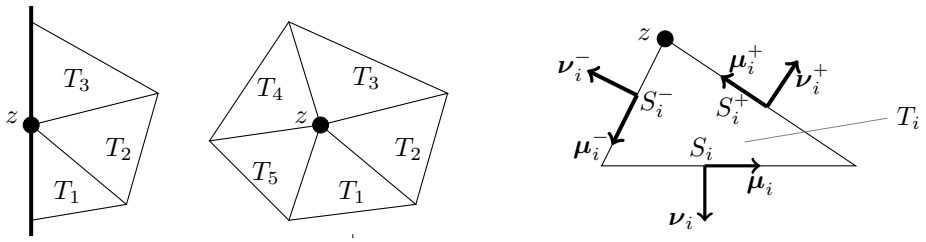

FIG. 5.1. *Notation in* (5.1)*: ω_z is formed by $\{T_i\}_{i=1}^{N_z}$ with $N_z = 3$ (left) and $N_z = 5$ (centre); the edge S_i in T_i is opposite to z, with the outward normal and the counterclockwise tangential unit vectors $\boldsymbol{\nu}_i$ and $\boldsymbol{\mu}_i$; the other edges $S_i^{\pm} = \partial T_i \cap \partial T_{i\pm1}$ have the outward normal and the counterclockwise tangential unit vectors $\boldsymbol{\nu}_i^{\pm}$ and $\boldsymbol{\mu}_i^{\pm}$ (right).*

$T_i \in \mathcal{T}^*$ and $z = z^*_{T_i}$ so $\theta_{T_i;z} = 0$. Now, $|\varepsilon\alpha_i| \lesssim (h_z\varepsilon^{-1})\,\theta_{T_i;z}|\widetilde{F}_{T_i;z}|$. Combining this with (5.1b) and (3.7), one gets (5.2b)

Next, note that (4.4), combined with (5.1a), is equivalent to

$$\big(\alpha_{i-1}\boldsymbol{\nu}_{i-1} + \beta_{i-1}d_{i-1}^{-1}\boldsymbol{\mu}_{i-1}\big)\cdot\boldsymbol{\nu}_{i-1}^{+} + \big(\alpha_i\boldsymbol{\nu}_i + \beta_i d_i^{-1}\boldsymbol{\mu}_i\big)\cdot\boldsymbol{\nu}_i^{-} = \big[\partial_{\boldsymbol{\nu}}u_h\big]_{\partial T_{i-1}\cap\partial T_i}.$$

Multiplying this by $|S_{i-1}^+| = |S_i^-|$ and noting that $d_i = \boldsymbol{\mu}_i\cdot|S_i^+|\boldsymbol{\nu}_i^+ = -\boldsymbol{\mu}_i\cdot|S_i^-|\boldsymbol{\nu}_i^-$, one gets (5.1c). So (5.1c) is, indeed, equivalent to (4.4).

Finally, consider the system (5.1c) for $\{\beta_i\}_{i=1}^{N_z}$. For $z \in \partial\Omega$, there are $N_z - 1$ equations, so this system is clearly under-determined. For $z \notin \partial\Omega$, this is also the case as an application of $\sum_{i=1}^{N_z}$ to (5.1c) yields 0. To check the latter, one first employs the observation that $\boldsymbol{\nu}_i\cdot\big(|S_i^+|\boldsymbol{\nu}_i^+ + |S_i^-|\boldsymbol{\nu}_i^-\big) + 2|T_i|d_i^{-1} = 0$, and then recalls (5.1b), as well as (3.6) and (3.7). ∎

*Remark 5.2 (*Anisotropic flux equilibration*). The choice of a particular solution $\{\beta_i\}$ of* (5.1c) *is crucial, as our estimator, roughly speaking, involves the component $\sum_{i=1}^{N_z}\beta_i^2 d_i^{-2}|T_i|$ from* (5.2b)*, while, unless the mesh is shape-regular, $d_i^{-2}|T_i| = \frac{1}{4}|S_i|^2|T_i|^{-1}$ may vary very significantly within ω_z. One simple and useful approach is to minimize this component, i.e. given any particular solution $\{\hat\beta_i\}$ of* (5.1c)*, let*

$$\beta_i := \hat\beta_i - C_z, \qquad \text{where} \quad \sum_i(\hat\beta_i - C_z)d_i^{-2}|T_i| = 0. \tag{5.3}$$

(Alternatively, one can set $\beta_i := 0$ for the element T_i with the largest $d_i^{-2}|T_i|$ within ω_z, or choose $\{\beta_i\}$ as in the proof of Lemma 5.4.)

5.1. Proof of (4.7) **and** (4.8) **in Theorem 4.3(i) for $h_z \lesssim \varepsilon$.** Our findings in this section are presented as two lemmas.

LEMMA 5.3. *Let $\{\boldsymbol{\tau}_z\}$ satisfy* (5.1a), (5.1b) *for any $z \in \mathcal{N}$ with $h_z \lesssim \varepsilon$. Then for any $z \in \mathcal{N}$, there is a function g_z with support on ω_z that satisfies* (4.7) *and* (4.8)*.*

Proof. In any $T \subset \omega_z$, let $g_z := \varepsilon^2\mathrm{div}\boldsymbol{\tau}_z + \theta_{T;z}F_{T;z}$ if $h_z \lesssim \varepsilon$, and $g_z := \theta_{T;z}F_{T;z}$ otherwise. In view of (3.2), (3.6), $\sum_{\mathcal{N}\cap z\in\partial T}\theta_{T;z}F_{T;z} = \bar f_{h;T} = \bar f_h$ in any $T \in \mathcal{T}$, so the first assertion (4.7) follows. Next, if $h_z \gtrsim \varepsilon$, i.e. $\min\{1, h_z\varepsilon^{-1}\} \simeq 1$, one immediately gets $\|g_z\|_{\omega_z} \lesssim \min\{1, h_z\varepsilon^{-1}\}\|f_h^I\|_{\omega_z}$. Otherwise, i.e. if $h_z \lesssim \varepsilon$, (5.2a) implies $|g_z| \leqslant |F_{T;z} - \widetilde{F}_{T;z}|$ for any $T \subset \omega_z$. By (5.1b), unless $g_z = 0$, one has $|g_z| \leqslant |F_{T;z} - \bar F_z| \leqslant \mathrm{osc}(f_h^I;\omega_z)$, where we also used (3.7). At the same time, $H_z \gtrsim \varepsilon$ implies $1 \simeq \min\{1, H_z\varepsilon^{-1}\} \simeq \lambda_T$ (as $z \in \mathcal{N}_{\mathrm{ani}}$ so $H_z \simeq H_T$). Combining these observations with $|T| \simeq |\omega_z|$ for any $T \subset \omega_z$ yields $\|g_z\|_{\omega_z} \lesssim \sum_{T\subset\omega_z}\lambda_T\|\mathrm{osc}(f_h^I;T)\|_T$. ∎

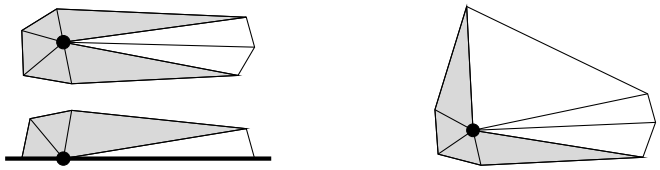

FIG. 5.2. *Examples of nodes that satisfy $\mathcal{A}1_{\rm mix}$ with the set $\{T_i\}_{i=1}^n$ (used in the proof of Lemma 5.4) highlighted by the grey color: $n=5$ (top left), $n=3$ (bottom left), $n=4$ (right).*

LEMMA 5.4. *Under condition $\mathcal{A}1$, for any $z\in\mathcal{N}$ with $h_z\lesssim\varepsilon$, there is a solution $\{\beta_i\}_{i=1}^{N_z}$ of* (5.1c) *such that $\boldsymbol{\tau}_z$ defined by* (5.1) *satisfies* (4.8).

Proof. Our task is to show that $\|\varepsilon\boldsymbol{\tau}_z\|_{\omega_z}$ satisfies (4.8), in which the right-hand side involves $\min\{1,\,h_z\varepsilon^{-1}\}\simeq h_z\varepsilon^{-1}$ and $\lambda'_T=\min\{1,\,\varepsilon H_T h_T^{-2}\}\simeq 1$. (The latter follows from $H_T\geqslant h_T$ combined with $\varepsilon\gtrsim h_z\geqslant h_T$.) So it suffices to prove that

$$\|\varepsilon\boldsymbol{\tau}_z\|_{\omega_z}\lesssim\|\varepsilon J_z\|_{\omega_z}+h_z\varepsilon^{-1}\|f_h^I\|_{\omega_z}+\sum_{T\subset\omega_z}\lambda_T\|\mathrm{osc}(f_h^I;T)\|_T+\mathbb{1}_{z\in\mathcal{N}_{\partial\Omega}^*}\|\lambda_T f_h(z)\|_{\omega_z}. \quad (5.4)$$

An inspection of the proof of Lemma 5.1 reveals that if $\widetilde{F}_{T;z}=F_{T;z}$ in (5.1b), then

$$\sum_{T_i\subset\omega_z}\|\varepsilon\alpha_i\|_{\omega_z}^2\lesssim|\omega_z|\,|h_z\varepsilon^{-1}f_h(z)|^2+|\omega_z|\sum_{\substack{T_i\in\mathcal{T}^*:\\ d_i\simeq h_{T_i}}}|d_i\varepsilon^{-1}\bar{f}_{h;T}|^2\lesssim\sum_{T\subset\omega_z}\|h_z\varepsilon^{-1}f_h^I\|_T^2,$$

where for the first relation we used (3.6) combined with (3.2), (3.3), and for the second, $|\omega_z|\simeq h_zH_z$ and $h_{T_i}H_z\simeq|T_i|$ for any $T_i\in\mathcal{T}^*$. One gets a similar conclusion for the case $\widetilde{F}_{T;z}=\bar{F}_z$ in (5.1b) (in fact, the latter case is more straightforward as then $z\in\mathcal{N}_{\rm ani}$ so $|T_i|\simeq|\omega_z|$ for any $T_i\subset\omega_z$). Now, in view of (5.2b), to get the desired assertion (5.4), it suffices to show that

$$|\beta_i d_i^{-1}|\lesssim|J_z|+\max_{j=1,\dots,N_z}|\alpha_j|+|\hat{\sigma}_z|, \quad (5.5)$$

with some $\hat{\sigma}_z$ such that $\|\varepsilon\hat{\sigma}_z\|_{\omega_z}$ satisfies a version of (5.4).

For (5.5), we start with a straightforward observation that follows from (5.1c):

$$\text{if }\ |S_i^-|\simeq d_i\gtrsim d_{i-1}\quad\Rightarrow\quad|\beta_i d_i^{-1}|\lesssim|\beta_{i-1}d_{i-1}^{-1}|+|\alpha_{i-1}|+|\alpha_i|+|J_z|. \quad (5.6)$$

Consider three cases (a), (b) and (c).

(a) Suppose that z satisfies $\mathcal{A}_{\rm mix}$. Then the N_z triangles in ω_z can be numbered counterclockwise so that the set $\{T_i\}_{i=1}^n\neq\varnothing$, with some $n=n_z\leqslant N_z$, is formed by all triangles having at least one edge in $\mathring{S}_z$ (see Fig. 5.2). To be more precise, this set will include all triangles from $\mathring{\omega}_z$, and, possibly, one or two anisotropic triangles that either share an edge with $\mathring{\omega}_z\neq\varnothing$ or, if $\mathring{\omega}_z=\varnothing$ and so $\mathring{S}_z$ includes a single edge, touch this edge. Note that then $d_i\simeq\mathring{h}_z$ for $i=1,\dots,n_z$ and $d_i\simeq H_z$ for $i>n_z$, while $|S_i^-|\simeq\mathring{h}_z$ for $i=2,\dots,n_z$. So setting $\beta_1:=0$ and applying (5.6) for $i>1$, we arrive at (5.5) with $\hat{\sigma}_z:=0$.

(b) Next, consider $z\in\mathcal{N}_{\rm ani}\backslash\partial\Omega$ that satisfies $\mathcal{A}1_{\rm ani}$ (and so not $\mathcal{A}1_{\rm mix}$). Then $\mathring{\mathcal{S}}_z$ includes exactly two edges of length $\simeq\mathring{h}_z\simeq h_z$. Let the triangles $\{T_i\}_{i=1}^N$ forming the patch ω_z be numbered counterclockwise so that $\mathring{\mathcal{S}}_z=\{\partial T_{i-1}\cap\partial T_i\}_{i=1,m+1}$, for some $m=m_z\leqslant N_z-2$ (see Fig. 5.3 (left)).

Note that $d_i \simeq h_z$ only for $i = 0, 1, m, m+1$ and $d_i \simeq H_z$ otherwise, while $|S_i^-| \simeq h_z$ for $i = 1, m$ and $\simeq H_z$ otherwise. Hence, one can employ (5.6) for $i \neq 0, m$. So it remains to get the desired bound (5.5) only for $i = 0, m$. For this, let

$$\widetilde{\sigma}_z := \sum_{i=2}^{m} |S_i^-| \big[\partial_{\boldsymbol{\nu}} u_h\big]_{\partial T_{i-1} \cap \partial T_i} + 2\varepsilon^{-2} \sum_{i=1}^{m} \theta_{T_i;z} |T_i| \, \widetilde{F}_{T_i;z} \tag{5.7}$$

(compare with (3.6)). Now, an application of $\sum_{i=1}^{m}$ to (5.1c) (and also noting that $\boldsymbol{\nu}_i \cdot \big(|S_i^+| \boldsymbol{\nu}_i^+ + |S_i^-| \boldsymbol{\nu}_i^-\big) + 2|T_i| d_i^{-1} = 0$) yields

$$\beta_0 - \beta_m + \alpha_0 \boldsymbol{\nu}_0 \cdot |S_0^+| \boldsymbol{\nu}_0^+ - \alpha_m \boldsymbol{\nu}_m \cdot |S_m^+| \boldsymbol{\nu}_m^+ = |S_1^-| \big[\partial_{\boldsymbol{\nu}} u_h\big]_{\partial T_0 \cap \partial T_1} + \widetilde{\sigma}_z. \tag{5.8}$$

So, for example, one can set $\beta_0 := 0$ and compute and then estimate β_m from (5.8). Or, one can choose β_0 and β_m, in agreement with (5.8), but in a more balanced way. Importantly, one can ensure for $i = 0, m$ that $|\beta_i d_i^{-1}| \lesssim |\alpha_i| + |J_z| + h_z^{-1} |\widetilde{\sigma}_z|$. Consequently, we get (5.5) for all i with $\hat{\sigma}_z := h_z^{-1} \widetilde{\sigma}_z$.

Finally, similarly to (3.7), define a version of (5.7):

$$\sigma_z := \sum_{i=2}^{m} |S_i^-| \big[\partial_{\boldsymbol{\nu}} u_h\big]_{\partial T_{i-1} \cap \partial T_i} + 2\varepsilon^{-2} \bar{F}_z \sum_{i=1}^{m} \theta_{T_i;z} |T_i|. \tag{5.9}$$

By (5.1b), unless $\widetilde{\sigma}_z = \sigma_z$, one has $\widetilde{F}_{T_i;z} \neq \bar{F}_z$ and so $H_z \varepsilon^{-1} \simeq \min\{1, H_z \varepsilon^{-1}\} \simeq \lambda_T$ (the latter is also because $z \in \mathcal{N}_{\rm ani}$), so $\varepsilon h_z^{-1} |\widetilde{\sigma}_z - \sigma_z| \lesssim \sum_{T \subset \omega_z} \lambda_T \operatorname{osc}(f_h^I; T)$. Combining this with a technical result (5.12) (obtained below in §5.2), one arrives at

$$|\varepsilon \hat{\sigma}_z| \lesssim |\varepsilon J_z| + h_z \varepsilon^{-1} |\bar{F}_z| + \sum_{T \subset \omega_z} \lambda_T \operatorname{osc}(f_h^I; T). \tag{5.10}$$

As $\|\bar{F}_z\|_{\omega_z} \lesssim \|f_h^I\|_{\omega_z}$ (by (3.6), (3.7)), so we have again obtained (5.5) with $\|\varepsilon \hat{\sigma}_z\|_{\omega_z}$ now satisfying a version of (5.4). This completes the proof of (5.4) for this case.

(c) It remains to consider $z \in \mathcal{N}_{\partial\Omega}^*$ that satisfies $\mathcal{A}1_{\rm ani}$ but not $\mathcal{A}1_{\rm mix}$. This case is similar to case (b), with a version of (5.8) becoming

$$\beta_1 - \beta_m - \alpha_1 \boldsymbol{\nu}_1 \cdot |S_1^-| \boldsymbol{\nu}_1^- - \alpha_m \boldsymbol{\nu}_m \cdot |S_m^+| \boldsymbol{\nu}_m^+ = \widetilde{\sigma}_z.$$

Again, using (5.12), we get a version of (5.10) with an additional term $H_z \varepsilon^{-1} |\bar{F}_z|$ in the right-hand side. As, by (3.7), $\bar{F}_z = f_h(z)$ for $z \in \partial\Omega$, we again get (5.4), only with $\lambda_T f_h(z)$ replaced by $f_h(z)$.

To address this deficiency, note that all our arguments remain valid independently of the values of f_h^I on the boundary. Hence a version of (5.4) remains true with f_h^I replaced by $\widetilde{f}_h^I := f_h^I - \sum_{z \in \mathcal{N}_{\partial\Omega}^*} \phi_z f_h(z)$, as well as $\lambda_T f_h(z)$ replaced by $\widetilde{f}_h^I(z) = 0$. Furthermore, in the latter bound, $|\widetilde{f}_h^I| + \operatorname{osc}(\widetilde{f}_h^I; T) \lesssim |f_h(z)| + \operatorname{osc}(f_h^I; T)$ and $h_z \varepsilon^{-1} \lesssim \min\{1, h_z \varepsilon^{-1}\} \lesssim \lambda_T$. These observations complete the proof of (5.4) for $z \in \mathcal{N}_{\partial\Omega}^*$. □

5.2. Estimation of σ_z. Here we give one technical result on σ_z. Throughout this section, we use the notation from the proof of Lemma 5.4.

LEMMA 5.5. *(i) If $z \in \mathcal{N}_{\rm ani} \backslash \partial\Omega$, with $h_z \lesssim \varepsilon$, satisfies $\mathcal{A}1_{\rm ani}^*$, then for σ_z of (5.9) one has*

$$\varepsilon h_z^{-1} \bigg| \sigma_z - \sum_{i=1,m+1} \boldsymbol{\mu}_{i-1}^+ \cdot \mathbf{i}_\xi \, \frac{H_{T_{i-1}} H_{T_i}}{H_{T_{i-1}} + H_{T_i}} \big[\partial_{\boldsymbol{\nu}} u_h\big]_{\partial T_{i-1} \cap \partial T_i} \bigg| \lesssim |\varepsilon J_z| + h_z \varepsilon^{-1} |\bar{F}_z|, \tag{5.11}$$

where $\mathbf{i}_\xi$ is the unit vector that points from z in the direction of any edge from $\{S_i^-\}_{i=2}^m$.

(ii) If $z \in \mathcal{N}_{\rm ani}\backslash\{$corners of $\Omega\}$, with $h_z \lesssim \varepsilon$, satisfies $\mathcal{A}1_{\rm ani}$ but not $\mathcal{A}1_{\rm mix}$, then

$$\varepsilon h_z^{-1}|\sigma_z| \lesssim |\varepsilon J_z| + h_z\varepsilon^{-1}|\bar F_z| + \mathbb{1}_{z\in\mathcal{N}^*_{\partial\Omega}}\, H_z\varepsilon^{-1}|\bar F_z|. \tag{5.12}$$

Proof. (i) For any scalar w, let $[\![w]\!]_{\partial T_{i-1}\cap\partial T_i} := w\big|_{\partial T_i} - w\big|_{\partial T_{i-1}}$. Furthermore, for fixed $z\in\mathcal{N}$, introduce the local cartesian coordinates (ξ,η) such that $z=(0,0)$, and $\mathbf{i}_\xi$ points in the ξ direction (see Fig. 5.3 (left)). In these coordinates, let (ξ_i,η_i) be the endpoint of the edge $S_i^- = \partial T_{i-1}\cap\partial T_i$ on $\partial\omega_z$.

Now, a calculation shows that $|S_i^-|\big[\partial_{\boldsymbol\nu}u_h\big]_{\partial T_{i-1}\cap\partial T_i} = \eta_i[\![\partial_\xi u_h]\!] - \xi_i[\![\partial_\eta u_h]\!]$, where, by $\mathcal{A}^*_{\rm ani}$ and the maximum angle condition, any $|\eta_i|\lesssim h_z$, while $H_z^+ := \min\limits_{i=2,\dots m}\xi_i \simeq H_z$ and $0\leqslant \xi_i - H_z^+ \lesssim h_z$, so

$$\sigma_z = -\sum_{i=2}^m H_z^+[\![\partial_\eta u_h]\!]_{\partial T_{i-1}\cap\partial T_i} + \mathcal{O}(h_z|J_z|) + \varepsilon^{-2}\bar F_z\sum_{i=1,m}|T_i|. \tag{5.13}$$

Here we also used $\theta_{T_i;z}=0$ for $i=2,\dots,m-1$ and $\theta_{T_i;z}=\frac12$ for $i=1,m$ in view of $T_i\subset\mathcal{T}^*$ for any $T_i\subset\omega_z$ (see also (3.2), (3.3)).

Next, multiplying (3.6) combined with (3.7) by $2\varepsilon^{-2}$, then subtracting σ_z and applying a similar argument, one gets

$$-\sigma_z = \sum_{i=m+2}^N H_z^-[\![\partial_\eta u_h]\!]_{\partial T_{i-1}\cap\partial T_i} + \mathcal{O}(h_z|J_z|) + \varepsilon^{-2}\bar F_z\sum_{i=m+1,N}|T_i|. \tag{5.14}$$

Here $H_z^- := \min\limits_{i=m+2,\dots N}|\xi_i| \simeq H_z$, and we also used $|S_i^-|\simeq h_z$ for $i=1,m+1$.

Finally, using $|T_1| = \frac12|\xi_2\eta_1-\xi_1\eta_2| = \frac12\eta_1H_z^+ + \mathcal{O}(h_z^2)$ (where $|\xi_1|+|\eta_2|\lesssim h_z$) and similar observations for the other triangle areas, we arrive at

$$\sum_{i=1,m}H_z^-|T_i| - \sum_{i=m+1,N}H_z^+|T_i| = \mathcal{O}(h_z^2H_z).$$

Combining this with (5.13), (5.14) and $\sum_{i=1}^N[\![\partial_\eta u_h]\!]_{\partial T_{i-1}\cap\partial T_i}=0$ yields

$$(H_z^- + H_z^+)\sigma_z = \sum_{i=1,m+1}H_z^-H_z^+\,[\![\partial_\eta u_h]\!]_{\partial T_{i-1}\cap\partial T_i} + h_zH_z\,\mathcal{O}\big(|J_z| + h_z\varepsilon^{-2}|\bar F_z|\big).$$

The desired assertion (5.11) follows in view of $H_z^+ = H_{T_i} + \mathcal{O}(h_z)$ for $i=1,m$ and a similar relation with H_z^- for $i=m+1,N$, as well as

$$[\![\partial_\eta u_h]\!]_{\partial T_{i-1}\cap\partial T_i} = \boldsymbol\mu_{i-1}^+\cdot\mathbf{i}_\xi\;[\partial_{\boldsymbol\nu}u_h]_{\partial T_{i-1}\cap\partial T_i}\,.$$

The latter follows from $\partial_\eta = \mathbf{i}_\eta\cdot\nabla$ combined with $[\![\nabla u_h]\!]_{\partial T_{i-1}\cap\partial T_i} = \boldsymbol\nu_i^-[\partial_{\boldsymbol\nu}u_h]_{\partial T_{i-1}\cap\partial T_i}$ and $\boldsymbol\nu_i^-\cdot\mathbf{i}_\eta = \boldsymbol\mu_{i-1}^+\cdot\mathbf{i}_\xi$.

(ii) If $z\in\mathcal{N}_{\rm ani}\backslash\partial\Omega$, then $\mathcal{A}1$ implies $|\boldsymbol\mu_{i-1}^+\cdot\mathbf{i}_\xi|\lesssim h_zH_z^{-1}$, so (5.11) implies (5.12). It remains to consider $z\in\mathcal{N}^*_{\partial\Omega}$. In view of $\mathcal{A}1$ and (2.4), one may choose the unit vector $\mathbf{i}_\xi$ in part (i) of this proof to be normal to $\partial\Omega$. As $u_h=\partial_\eta u_h=0$ on $\partial\Omega$ so $\sum_{i=2}^m[\![\partial_\eta u_h]\!]_{\partial T_{i-1}\cap\partial T_i}=0$, so (5.13) again yields the desired assertion (5.12). ∎

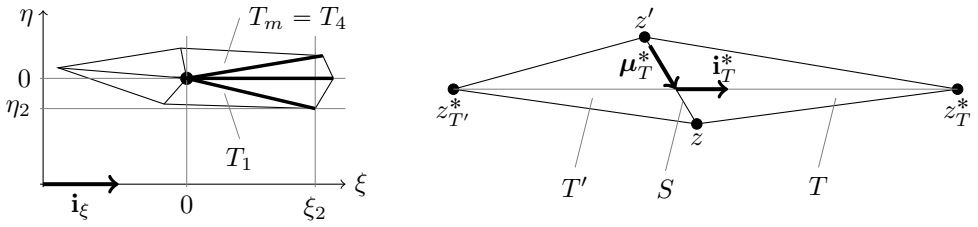

FIG. 5.3. *Notation used in Lemma 5.5 (left): the edges* $\{S_i^-\}_{i=2}^m$ *(here* $m = 4$*) are highlighted, the unit vector* $\mathbf{i}_\xi$ *in the direction of any of these edges (here* S_3^-*), local coordinates* (ξ, η)*, the endpoint* (ξ_2, η_2) *of the edge* S_2^-*. Notation used in the definition* (6.2) *of* $\boldsymbol{\tau}_S^J$ *(right).*

6. Construction of $\boldsymbol{\tau}_z$ for $h_z \lesssim \varepsilon$ under weaker condition $\mathcal{A}1^*$. Proof of Theorem 4.3(ii). This section deals with a weaker version $\mathcal{A}1^*$ of $\mathcal{A}1$. For this we need to address the terms subtracted from σ_z in (5.11) (which are $\lesssim h_z|J_z|$ under assumption $\mathcal{A}1$, but not under $\mathcal{A}1^*$).

Let $\mathcal{S}^*$ in the definition (4.3) of $\boldsymbol{\tau}$ be

$$\mathcal{S}^* := \big\{S \in \mathcal{S} \ : \ S = \partial T \cap \partial T', \ \ |S| \simeq h_T \lesssim \varepsilon, \ \ h_T \simeq h_{T'} \ll H_T \simeq H_{T'}\big\}. \tag{6.1}$$

Roughly speaking, $\mathcal{S}^* \subset \mathcal{S}$ is the set of short edges shared by pairs of anisotropic triangles. Now, we include a non-trivial component $\sum_{S\in\mathcal{S}^*} \boldsymbol{\tau}_S^J$ in $\boldsymbol{\tau}$, where $\boldsymbol{\tau}_S^J$ has support on $T \cup T'$ for any $S = \partial T \cap \partial T' \in \mathcal{S}^*$, and

$$\boldsymbol{\tau}_S^J := \kappa_T (d_T^*)^{-1}(\phi_z + \phi_{z'})\boldsymbol{\mu}_T^* \ \text{ in } T, \qquad \kappa_T = \kappa_{T'} := \boldsymbol{\mu}_T^* \cdot \mathbf{i}_T^* \ \frac{H_T H_{T'}}{H_T + H_{T'}} \, [\partial_{\boldsymbol{\nu}} u_h]_S \, . \tag{6.2}$$

Here $d_T^* := 2|T||S|^{-1}$, $\boldsymbol{\mu}_T^*$ is the tangential unit vector along S in the counterclockwise direction in T, the edge S joins the nodes z' and z, with $\boldsymbol{\mu}_T^*$ pointing from z' to z, and $\mathbf{i}_T^*$ is the unit vector in the direction from $z_{T'}^*$ to z_T^*, the latter being the vertices opposite to S in T' and T respectively; see Fig. 5.3 (right). Note that $\boldsymbol{\mu}_T^* = -\boldsymbol{\mu}_{T'}^*$ and $\mathbf{i}_T^* = -\mathbf{i}_{T'}^*$ so the definitions of κ_T and $\kappa_{T'}$ are consistent.

LEMMA 6.1. *For any* $S = \partial T \cap \partial T' \in \mathcal{S}^*$ *with the notation* (6.1), (6.2)*, one has* (4.10) *and*

$$\boldsymbol{\tau}_S^J \cdot \boldsymbol{\nu} = 0 \ \text{ on } S, \qquad |S''|\boldsymbol{\tau}_S^J \cdot \boldsymbol{\nu} = \kappa_T(\phi_z - \phi_{z'}) \ \text{ on any edge } S'' \subset \partial T \backslash S. \tag{6.3}$$

Proof. For $\mathrm{div}\boldsymbol{\tau}_S^J = 0$ in (4.10), as well as (6.3), imitate the proof of Lemma 5.1. For the final assertion in (4.10), see the proof of Lemma 5.4. Finally, for the bound on $\varepsilon\boldsymbol{\tau}_S^J$ in (4.10), note that $d_T^* \simeq d_{T'}^* \simeq H_T$ implies $|\boldsymbol{\tau}_S^J| \lesssim H_T^{-1}|\kappa_T| \lesssim |[\partial_{\boldsymbol{\nu}} u_h]_S|$. ∎

Now that $\sum_{S\in\mathcal{S}^*} \boldsymbol{\tau}_S^J$ is included in $\boldsymbol{\tau}$, we need to ensure that $\boldsymbol{\tau}$ still satisfies (4.1). For this, the definition of $\boldsymbol{\tau}_z$ should be updated to take into account the possibly non-trivial jumps $[\boldsymbol{\tau}_S^J \cdot \boldsymbol{\nu}]$ across γ_z. Note that we do not need to modify $\boldsymbol{\tau}_z$ if, under condition $\mathcal{A}2$, $h_z \gtrsim \varepsilon$, as then $h_T \gtrsim \varepsilon$ implies $\gamma_z \cap \mathcal{S}^* = \varnothing$.

For $h_z \lesssim \varepsilon$, the definition (5.1) of $\boldsymbol{\tau}_z$ is tweaked as follows. Relations (5.1a) and (5.1b) remain unchanged, while in (5.1c) we replace $\{\beta_i\}_{i=1}^{N_z}$ by $\{\beta_i^*\}_{i=1}^{N_z}$, where

$$\beta_i^* := \begin{cases} \beta_i - \kappa_{T_i} & \text{if } \ \partial T_i \cap \gamma_z \cap \mathcal{S}^* \neq \varnothing, \\ \beta_i & \text{otherwise.} \end{cases} \tag{6.4}$$

*Remark 6.2 (*Anisotropic flux equilibration*). The observations of Remark 5.2 remain valid (although a version of system* (5.1c) *is now solved for* $\{\beta_i^*\}$ *). One can simply use* (5.3) *(or choose* $\{\beta_i\}$ *as in the proof of Lemma 6.3).*

LEMMA 6.3. *Under condition* $\mathcal{A}1^*$*, for any* $z \in \mathcal{N}$ *with* $h_z \lesssim \varepsilon$*, let* $\boldsymbol{\tau}_z$ *be defined by* (5.1a) *and* (5.1b) *and use the notation* (6.1), (6.2)*. Then there is a solution of the system* (5.1c)*, in which* $\{\beta_i\}_{i=1}^{N_z}$ *is replaced by* $\{\beta_i^*\}_{i=1}^{N_z}$ *of* (6.4)*, such that* $\boldsymbol{\tau}$ *of* (4.3) *satisfies* (4.1) *and the results of Lemmas 5.1, 5.3 and 5.4 remain true.*

Proof. One can easily check that, indeed, the results of Lemmas 5.1 and 5.3 remain true, while for Lemma 5.4, it suffices to obtain (5.5). That the normal jumps in $\boldsymbol{\tau}$ satisfy (4.1) can be checked by a direct calculation using (6.3) and taking into account that if $(\partial T_{i-1} \cap \partial T_i) \subset (\gamma_z \cap \mathcal{S}^*)$, then $\beta_i - \beta_{i-1} = \beta_i^* - \beta_{i-1}^*$ (in view of $\kappa_{T_{i-1}} = \kappa_{T_i}$). Note that in the latter case (5.6) is still true.

Otherwise, i.e. for $(\partial T_{i-1} \cap \partial T_i) \not\subset (\gamma_z \cap \mathcal{S}^*)$, a version of (5.6) will be employed:

$$\text{if } |S_i^-| \simeq d_i \gtrsim d_{i-1} \;\Rightarrow\; |\beta_i d_i^{-1}| \lesssim |\beta_{i-1} d_{i-1}^{-1}| + \max_j |\alpha_j| + \max_{\partial T \cap \gamma_z \cap \mathcal{S}^* \neq \varnothing} |\kappa_T| d_i^{-1} + |J_z|. \tag{6.5}$$

Next, consider two cases (a) and (b), as in the proof of Lemma 5.4, to get the bound (5.5) for $\beta_i d_i^{-1}$ and thus complete the proof.

(a) Suppose that z satisfies $\mathcal{A}_{\rm mix}$. Unless $\gamma_z \cap \mathcal{S}^* = \varnothing$ (and so the results of Lemma 5.4 apply), $\mathring{\omega}_z = \varnothing$ and $\mathring{\mathcal{S}}_z = \gamma_z \cap \mathcal{S}^*$ contains exactly one edge $\partial T_1 \cap \partial T_2$. Set $\beta_1 := 0$ and use (5.6) with $i = 2$ as in the proof of Lemma 5.4. For $i > 2$, use (6.5), where $d_i \simeq H_z$, so the additional term $|\kappa_T| d_i^{-1} \lesssim |\kappa_{T_2}| H_z^{-1} \lesssim |J_z|$. So we get (5.5) with $\hat{\sigma}_z := 0$.

(b) It remains to consider $z \in \mathcal{N}_{\rm ani} \backslash \partial\Omega$ under condition $\mathcal{A}1^*_{\rm ani}$ (as $z \in \mathcal{N}_{\rm ani} \cap \partial\Omega$ satisfies either $\mathcal{A}1_{\rm ani}$ or $\mathcal{A}1_{\rm mixed}$, so have been considered in part (a) or in Lemma 5.4). We shall imitate part (b) from the proof of Lemma 5.4. Note that $(\partial T_{i-1} \cap \partial T_i) \subset (\gamma_z \cap \mathcal{S}^*)$ only for $i = 1, m+1$. Hence, we employ (5.6) for $i = 1, m+1$, and (6.5) with $d_i \simeq H_z$ for $i \neq 1, m, m+1, N$, and it remains to bound $\beta_i d_i^{-1}$ for $i = 0, m$. For the latter, combining (5.8) with (6.4) yields

$$[\beta_0 - \kappa_{T_0}] - [\beta_m - \kappa_{T_m}] = \widetilde{\sigma}_z + \mathcal{O}\big(h_z |J_z|\big).$$

From this bound, one gets (5.5) only now $\hat{\sigma}_z := h_z^{-1}(\widetilde{\sigma}_z + \kappa_{T_0} - \kappa_{T_m})$. As $|\widetilde{\sigma}_z - \sigma_z|$ was bounded in the proof of Lemma 5.4, to complete the proof, it finally remains to show that

$$\varepsilon h_z^{-1} |\sigma_z + \kappa_{T_0} - \kappa_{T_m}| \lesssim |\varepsilon J_z|.$$

The above follows from (5.11) using the following observations. For κ_{T_0}, we use the edge $\partial T_0 \cap \gamma_z \cap \mathcal{S}^* = \partial T_0 \cap \partial T_1$ and $\boldsymbol{\mu}_{T_0}^* = \boldsymbol{\mu}_0^+$, while $|\mathbf{i}_{T_0}^* + \mathbf{i}_\xi| \lesssim h_z H_z^{-1}$. Similarly, for κ_{T_m}, we use the edge $\partial T_m \cap \gamma_z \cap \mathcal{S}^* = \partial T_m \cap \partial T_{m+1}$ and $\boldsymbol{\mu}_{T_m}^* = \boldsymbol{\mu}_m^+$, while $|\mathbf{i}_{T_m}^* - \mathbf{i}_\xi| \lesssim h_z H_z^{-1}$. ∎

7. Construction of $\boldsymbol{\tau}_z$ for $h_z \gtrsim \varepsilon$ under condition $\mathcal{A}2$. Throughout this section, for any $T \subset \omega_z$, we use S_T, $\boldsymbol{\nu}_T$ and $\boldsymbol{\mu}_T$, as well as $S_T^\pm$, $\boldsymbol{\nu}_T^\pm$ and $\boldsymbol{\mu}_T^\pm$, defined as in §5 (see Fig. 5.1 (right)) only with subscript T in place of i when dealing with element T. We start with a useful technical result.

FIG. 7.1. *Notation used in Lemma 7.1: each triangle $T^\pm \subset T$ shares the edge $S_T^\pm$ with T and has another edge of length $\varepsilon' \simeq \varepsilon$ along $S_T^\mp$.*

LEMMA 7.1. *Let $h_T \geqslant \sqrt{6}\varepsilon$. For any triangle T with a vertex z, there exist two functions $\boldsymbol{\tau}_{z;T}^+$ and $\boldsymbol{\tau}_{z;T}^-$ in T such that*

$$\boldsymbol{\tau}_{z;T}^\pm \cdot \boldsymbol{\nu} = 0 \ \text{ on } \partial T \backslash S_T^\pm, \qquad \boldsymbol{\tau}_{z;T}^\pm \cdot \boldsymbol{\nu} = \phi_z \ \text{ on } S_T^\pm, \tag{7.1a}$$

$$\|\varepsilon \operatorname{div} \boldsymbol{\tau}_{z;T}^\pm\|_T^2 = \|\boldsymbol{\tau}_{z;T}^\pm\|_T^2 = \tfrac{1}{2\sqrt{6}}\varepsilon |S_T^\pm| \varsigma_{T;z}^{-1}, \qquad \varsigma_{z;T} := \sin \angle(S_T^-, S_T^+). \tag{7.1b}$$

Proof. Let $\varepsilon' := \sqrt{6}\varepsilon$ and, skipping the subscripts when there is no ambiguity, set

$$\boldsymbol{\tau}^+ := -\varsigma^{-1} \varphi_z^+ \boldsymbol{\mu}^-, \qquad \boldsymbol{\tau}^- := \varsigma^{-1} \varphi_z^- \boldsymbol{\mu}^+.$$

Here φ_z^+ is a barycentric coordinate in the triangle T^+ formed by the edge $S_T^+ = S^+$ and the point $z + \varepsilon' \boldsymbol{\mu}^-$ such that $\varphi_z^+\big|_z = 1$; see Fig. 7.1. Similarly, φ_z^- is a barycentric coordinate in the triangle T^- formed by the edge $S_T^- = S^-$ and the point $z - \varepsilon' \boldsymbol{\mu}^+$.

The boundary properties (7.1a) are satisfied as $\boldsymbol{\mu}^\pm \cdot \boldsymbol{\nu}^\pm = 0$ and $\varsigma = -\boldsymbol{\mu}^- \cdot \boldsymbol{\nu}^+ = \boldsymbol{\mu}^+ \cdot \boldsymbol{\nu}^-$. Next, using $|T^+| = \frac{1}{2}\varepsilon' |S^+| \varsigma$,

$$\|\boldsymbol{\tau}^+\|_T^2 = \tfrac{1}{6}\varsigma^{-2}|T^+| = \tfrac{1}{2\sqrt{6}}\varepsilon \varsigma^{-1} |S^+|,$$

while $\operatorname{div} \boldsymbol{\tau}^+ = -\varsigma^{-1} \partial_{\boldsymbol{\mu}^-} \varphi_z^+ = \varsigma^{-1} \varepsilon'^{-1}$ so $\|\varepsilon \operatorname{div} \boldsymbol{\tau}^+\|_T^2 = (\varepsilon/\varepsilon')^2 \varsigma^{-2} |T^+| = \|\boldsymbol{\tau}^+\|_T^2$. ∎

*Remark 7.2 (*Version of $\mathcal{A}2$*). In $\mathcal{A}2$, one can impose that each $z \in \mathcal{N}$ with $h_z \gtrsim \varepsilon$ satisfies $\mathring{h}_z \geqslant c'\varepsilon$ for any fixed positive constant c' (rather than $\mathring{h}_z \geqslant \sqrt{6}\varepsilon$). For this case, one can employ a version of the above lemma under the condition $h_T \geqslant c'\varepsilon$. Choosing $\varepsilon' := c'\varepsilon$ in the proof, one, indeed, arrives at the following version of* (7.1b)*:*

$$\|\varepsilon \operatorname{div} \boldsymbol{\tau}_{z;T}^\pm\|_T^2 = 6c'^{-2} \|\boldsymbol{\tau}_{z;T}^\pm\|_T^2 = (2c')^{-1} \varepsilon |S_T^\pm| \varsigma_{T;z}^{-1}\,.$$

7.1. Definition of $\boldsymbol{\tau}_z$ for $h_z \gtrsim \varepsilon$. Introduce a subset ω_z^* of ω_z:

$$\omega_z^* := \Big\{ T \subset \omega_z : |S_T| \simeq h_T \ll H_T \text{ and } \tfrac{h_T}{H_T} \lesssim \tfrac{\varepsilon}{h_T} \Big\}, \tag{7.2}$$

i.e. ω_z^* includes only triangles with extremely small angles at z, so $\omega_z \backslash \omega_z^* \neq \varnothing$ (see Fig. 7.2). Now, using $\boldsymbol{\tau}_{z;T}^\pm$ from Lemma 7.1, set

$$\boldsymbol{\tau}_z := \begin{cases} \frac{1}{2}\Big(\mathcal{J}_z\big|_{S_T^-} \boldsymbol{\tau}_{z;T}^- + \mathcal{J}_z\big|_{S_T^+} \boldsymbol{\tau}_{z;T}^+ \Big) & \text{for } \ T \subset \omega_z \backslash \omega_z^*, \\ \phi_z \, \beta_T d_T^{-1} \boldsymbol{\mu}_T, \ \ d_T := 2|T| \, |S_T|^{-1} & \text{for } \ T \subset \omega_z^*, \end{cases} \tag{7.3}$$

where, with the convention $[\partial_{\boldsymbol{\nu}} u_h]_{\partial\Omega} := 0$,

$$\mathcal{J}_z\big|_{S_T^\pm} := \begin{cases} \big[\partial_{\boldsymbol{\nu}} u_h\big]_{S_T^\pm} & \text{if } \ S_T^\pm \notin \partial\omega_z^*, \\ |S_T^\pm|^{-1} \displaystyle\sum_{S \in \gamma_{z;T}^\pm} |S| \big[\partial_{\boldsymbol{\nu}} u_h\big]_S & \text{otherwise.} \end{cases} \tag{7.4}$$

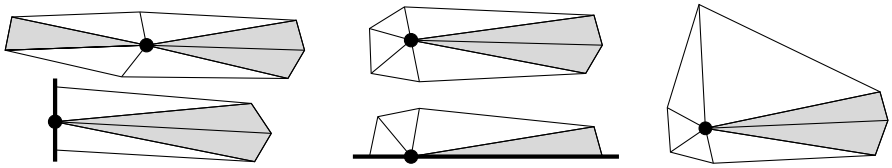

FIG. 7.2. *For various nodes, the set ω_z^* (defined by* (7.2)*) is highlighted by the grey color.*

To define $\gamma_{z;T}^{\pm}$ in (7.4), it is convenient to assume that ω_z^* includes triangles with their boundaries. Now, let $\omega_{z;T}^{\pm}$ be the maximal connected subset of $\omega_z^*\backslash\{z\}$ that shares the edge $S_T^{\pm}$ with T. The set of all edges originating at z that are contained in this subset $\omega_{z;T}^{\pm}$ (including $S_T^{\pm}$) is denoted $\gamma_{z;T}^{\pm}$.

The unique set of values $\{\beta_T\}$ for $T \subset \omega_z^*$ in (7.3) is chosen to satisfy (4.4). For example, consider a bundle of m triangles $\omega_{z;T}^{+} = \omega_{z;T'}^{-} = \{T_i\}_{i=1}^m$, numbered counterclockwise, that touches $T, T' \subset \omega_z\backslash\omega_z^*$. Now, (4.4) is equivalent to a version of (5.1c):

$$\beta_{i-1} - \beta_i = |S_i^-|[\partial_{\boldsymbol{\nu}} u_h]_{\partial T_{i-1}\cap\partial T_i}, \quad i = 1, \dots, m+1, \tag{7.5a}$$

where the notation $\beta_i := \beta_{T_i}$ is used for $i = 1, \dots, m$, while

$$\beta_0 = -\beta_{m+1} := \tfrac{1}{2}\sum_{i=1}^{m+1} |S_i^-|[\partial_{\boldsymbol{\nu}} u_h]_{\partial T_{i-1}\cap\partial T_i} = \tfrac{1}{2}|S_T^+|\,\mathcal{J}_z\big|_{S_T^+} = \tfrac{1}{2}|S_{T'}^-|\,\mathcal{J}_z\big|_{S_{T'}^-}. \tag{7.5b}$$

Note that the above system involves $m+1$ equations for $\{\beta_i\}_{i=1}^m$, but is consistent and has a unique solution. This becomes clear on application of $\sum_{i=1}^{m+1}$ to (7.5a) which yields a relation for $\beta_0 - \beta_{m+1}$ consistent with (7.5b).

If for a bundle of m triangles $\cup_{i=1}^m T_i = \omega_{z;T}^{+}$, numbered counterclockwise, one has $S_m^+ \subset \partial\Omega$, then we use (7.5a) with $i \neq m+1$, and β_0 from (7.5b) (while β_{m+1} remains undefined). Similarly, if $S_1^- \subset \partial\Omega$, then use (7.5a) with $i \neq 1$ combined with the definition of β_{m+1} from (7.5b) (and β_0 remaining undefined).

7.2. Proof of (4.8) **in Theorem 4.3 for** $h_z \gtrsim \varepsilon$**.** It suffices to prove the following.

LEMMA 7.3. *Under condition $\mathcal{A}2$, for any $z \in \mathcal{N}$ with $h_z \gtrsim \varepsilon$, the function $\boldsymbol{\tau}_z$ defined by* (7.1), (7.2) (7.3), (7.4), (7.5) *satisfies* (4.4) *and*

$$\|\varepsilon^2 \operatorname{div}\boldsymbol{\tau}_z\|_T + \|\varepsilon\boldsymbol{\tau}_z\|_T \lesssim \min\{1, \varepsilon H_T h_T^{-2}\}^{1/2}\, \|\varepsilon J_z\|_T\,. \tag{7.6}$$

Proof. Condition (4.4) is satisfied by the construction of $\boldsymbol{\tau}_z$ in §7.1, so it remains to establish (7.6). First, consider $T \subset \omega_z^*$. By (7.3), $\operatorname{div}\boldsymbol{\tau}_z = 0$ (see the proof of Lemma 5.1), while, by (7.2), $d_T \simeq H_T \simeq H_z$, and, by (7.5), $|\beta_T| \lesssim H_z|J_z|$. So $|\varepsilon\boldsymbol{\tau}_z| \lesssim |\varepsilon J_z|$, while $\frac{h_T}{H_T} \lesssim \frac{\varepsilon}{h_T}$ implies $\min\{1, \varepsilon H_T h_T^{-2}\} \simeq 1$. So one gets (7.6) for $T \subset \omega_z^*$.

Next, consider $T \subset \omega_z\backslash\omega_z^*$. Note that $|\mathcal{J}_z| \leqslant |J_z|$, which follows from (7.4) as $|S| \simeq |H_T|$ for all edges $S \in \gamma_{z;T}^{\pm}$ including $S_T^{\pm}$. Now, combining (7.3) with (7.1b) and $|S_T^{\pm}| \lesssim H_T$ yields

$$\|\varepsilon^2 \operatorname{div}\boldsymbol{\tau}_z\|_T^2 + \|\varepsilon\boldsymbol{\tau}_z\|_T^2 \lesssim \varepsilon H_T \varsigma_{z;T}^{-1}\, |\varepsilon J_z|^2 \lesssim \varepsilon \varsigma_{z;T}^{-1} h_T^{-1}\, \|\varepsilon J_z\|_T^2\,,$$

TABLE 8.1
Errors $|||u_h - u|||_{\varepsilon;\Omega}$ compared with the corresponding estimators $\mathcal{E}$.

N	$\varepsilon = 1$	$\varepsilon = 2^{-5}$	$\varepsilon = 2^{-10}$	$\varepsilon = 2^{-15}$	$\varepsilon = 2^{-20}$	$\varepsilon = 2^{-25}$	$\varepsilon = 2^{-30}$
	Errors $\|\|\|u_h - u\|\|\|_{\varepsilon;\Omega}$						
64	3.203e-2	5.204e-3	1.065e-3	6.734e-4	6.576e-4	6.571e-4	6.571e-4
128	1.602e-2	2.594e-3	4.534e-4	1.797e-4	1.641e-4	1.636e-4	1.636e-4
256	8.011e-3	1.296e-3	2.157e-4	5.533e-5	4.133e-5	4.081e-5	4.080e-5
512	4.006e-3	6.479e-4	1.062e-4	2.130e-5	1.071e-5	1.020e-5	1.019e-5
	Estimators (odd rows) & Effectivity Indices (even rows)						
64	3.301e-2	6.959e-3	1.324e-3	6.878e-4	6.581e-4	6.572e-4	6.571e-4
	1.031	1.337	1.243	1.021	1.001	1.000	1.000
128	1.647e-2	2.698e-3	5.993e-4	1.928e-4	1.645e-4	1.636e-4	1.636e-4
	1.028	1.040	1.322	1.073	1.003	1.000	1.000
256	8.232e-3	1.335e-3	2.914e-4	6.541e-5	4.178e-5	4.083e-5	4.080e-5
	1.028	1.030	1.351	1.182	1.011	1.000	1.000
512	4.115e-3	6.668e-4	1.446e-4	2.753e-5	1.115e-5	1.022e-5	1.019e-5
	1.027	1.029	1.361	1.292	1.041	1.001	1.000

where we also used $|T| \simeq h_T H_T$. Consider two cases (a) and (b). (a) If $\frac{h_T}{H_T} \lesssim \frac{\varepsilon}{h_T}$, then, by (7.2), $|S_T| \simeq H_T$ so $\varsigma_{z;T}^{-1} \simeq 1$, while, by $\mathcal{A}2$, $\varepsilon h_T^{-1} \lesssim 1$. Combining this with $1 \simeq \min\{1, \varepsilon H_T h_T^{-2}\}$, one again gets (7.6). (b) Otherwise, $\varsigma_{z;T}^{-1} \lesssim H_T h_T^{-1}$ so $\varepsilon\varsigma_{z;T}^{-1} h_T^{-1} \lesssim \varepsilon H_T h_T^{-2}$. Combining this with $\varepsilon H_T h_T^{-2} \simeq \min\{1, \varepsilon H_T h_T^{-2}\}$ yields (7.6) also for this case, and thus completes the proof. □

8. Numerical results. Our estimator is tested using a simple version of (1.1) with $\Omega = (0,1)^2$ and $f = u - F(x,y)$, where F is such that the unique exact solution $u = 4y\,(1-y)\,[\cos(\pi x/2) - (e^{-x/\varepsilon} - e^{-1/\varepsilon})/(1 - e^{-x/\varepsilon})]$ (the latter exhibits a sharp boundary layer at $x = 0$). We consider one a-priori-chosen layer-adapted mesh, as on Fig. 8.1, which is obtained by drawing diagonals from the tensor product of the Bakhvalov grid $\{\chi(\frac{i}{N})\}_{i=1}^{N}$ in the x-direction [5] and a uniform grid $\{\frac{j}{M}\}_{j=0}^{M}$ in the y-direction with $M = \frac{1}{2}N$. The continuous mesh-generating function $\chi(t) = t$ if $\varepsilon > \frac{1}{6}$; otherwise, $\chi(t) = 3\varepsilon \ln \frac{1}{1-2t}$ for $t \in (0, \frac{1}{2} - 3\varepsilon)$ and is linear elsewhere subject to $\chi(1) = 1$.

In our numerical experiments, we set $\mathcal{T}_0 := \varnothing$ in (3.3) and replace $\lesssim$ by $\leqslant$ in (3.3), (4.3), (7.2) and when dealing with the two cases $h_z \lesssim \varepsilon$ and $h_z \not\lesssim \varepsilon$. Also, we understand $a \ll b$ as $a \leqslant \frac{1}{5}b$ for any two quantities a and b (so, for example, (3.3) becomes $\mathcal{T}^* := \{T \in \mathcal{T} : h_T \leqslant \frac{1}{5}H_T \text{ and } h_T \leqslant \varepsilon\}$).

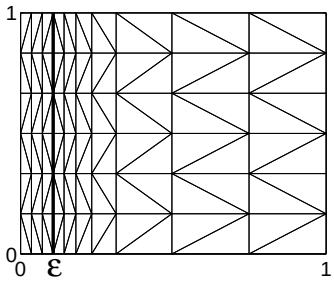

FIG. 8.1. *Triangulation used in Section 8 (similar meshes were considered in [13]).*

TABLE 8.2
Error component $\{\varepsilon^2\|\nabla u_h - (\nabla u)^I\|^2_{2;\Omega} + \|u_h - u^I\|^2_{2;\Omega}\}^{1/2}$ *from* (8.1) *compared with* $\mathcal{E}\big|_{f_h:=f_h^I}$.

N	$\varepsilon = 1$	$\varepsilon = 2^{-5}$	$\varepsilon = 2^{-10}$	$\varepsilon = 2^{-15}$	$\varepsilon = 2^{-20}$	$\varepsilon = 2^{-25}$	$\varepsilon = 2^{-30}$
	Errors (odd rows) & Computational Rates (even rows)						
64	3.203e-2	5.172e-3	8.450e-4	1.489e-4	2.632e-5	4.653e-6	8.225e-7
	1.000	0.997	0.996	0.996	0.996	0.996	0.996
128	1.602e-2	2.591e-3	4.237e-4	7.469e-5	1.320e-5	2.334e-6	4.126e-7
	1.000	0.999	0.999	0.998	0.998	0.998	0.998
256	8.011e-3	1.296e-3	2.119e-4	3.740e-5	6.611e-6	1.169e-6	2.066e-7
	1.000	1.000	1.003	0.999	0.999	0.999	0.999
512	4.006e-3	6.478e-4	1.057e-4	1.871e-5	3.308e-6	5.848e-7	1.034e-7
	Estimators (odd rows) & Effectivity Indices (even rows)						
64	3.290e-2	6.934e-3	1.158e-3	2.046e-4	3.617e-5	6.395e-6	1.130e-6
	1.027	1.341	1.370	1.374	1.374	1.374	1.374
128	1.646e-2	2.695e-3	5.787e-4	1.023e-4	1.808e-5	3.196e-6	5.650e-7
	1.027	1.040	1.366	1.369	1.370	1.370	1.370
256	8.230e-3	1.335e-3	2.893e-4	5.115e-5	9.042e-6	1.598e-6	2.826e-7
	1.027	1.030	1.365	1.368	1.368	1.368	1.368
512	4.115e-3	6.667e-4	1.446e-4	2.558e-5	4.522e-6	7.993e-7	1.413e-7
	1.027	1.029	1.368	1.367	1.367	1.367	1.367

TABLE 8.3
Error component $\|u - u^I\|_\Omega$ *from* (8.1) *compared with the estimator component* $\|f_h - f_h^I\|_\Omega$.

N	$\varepsilon = 1$	$\varepsilon = 2^{-5}$	$\varepsilon = 2^{-10}$	$\varepsilon = 2^{-15}$	$\varepsilon = 2^{-20}$	$\varepsilon = 2^{-25}$	$\varepsilon = 2^{-30}$
	Errors (odd rows) & Computational Rates (even rows)						
64	2.242e-4	6.120e-4	6.496e-4	6.567e-4	6.571e-4	6.571e-4	6.571e-4
	2.000	2.004	2.006	2.006	2.006	2.006	2.006
128	5.607e-5	1.525e-4	1.617e-4	1.635e-4	1.636e-4	1.636e-4	1.636e-4
	2.000	2.002	2.003	2.003	2.003	2.003	2.003
256	1.402e-5	3.807e-5	4.036e-5	4.077e-5	4.079e-5	4.080e-5	4.080e-5
	2.000	2.001	2.002	2.002	2.002	2.002	2.002
512	3.505e-6	9.510e-6	1.008e-5	1.018e-5	1.019e-5	1.019e-5	1.019e-5
	Estimators (odd rows) & Effectivity Indices (even rows)						
64	2.661e-3	5.762e-4	6.484e-4	6.567e-4	6.571e-4	6.571e-4	6.571e-4
	11.867	0.941	0.998	1.000	1.000	1.000	1.000
128	6.671e-4	1.435e-4	1.614e-4	1.634e-4	1.636e-4	1.636e-4	1.636e-4
	11.897	0.941	0.998	1.000	1.000	1.000	1.000
256	1.670e-4	3.579e-5	4.029e-5	4.077e-5	4.079e-5	4.080e-5	4.080e-5
	11.913	0.940	0.998	1.000	1.000	1.000	1.000
512	4.178e-5	8.938e-6	1.006e-5	1.018e-5	1.019e-5	1.019e-5	1.019e-5
	11.921	0.940	0.998	1.000	1.000	1.000	1.000

We compute the estimator $\mathcal{E}$ from (4.2) with $C_f := 1$ and $\boldsymbol{\tau}$ from (4.3), (4.6). As our mesh satisfies $\mathcal{A}1$ and $\mathcal{A}2$, we set $\mathcal{S}^* = \varnothing$. The component $\boldsymbol{\tau}_z$ in (4.3) is computed by (5.1) combined with (5.3) for $h_z \leqslant \varepsilon$, and, otherwise, using (7.2), (7.3), (7.4) combined with (7.5). Note that instead of explicitly including the components involving $\boldsymbol{\tau}^{\pm}_{z;T}$ (from (7.3)) in $\boldsymbol{\tau}$, we use (7.1b) (as well as Remark 7.2). This somewhat simplifies the computations, but yields a slightly less sharp estimator. When computing the error and the estimator, we replace ∇u by its linear Lagrange interpolant, and u and f_h by their quadratic Lagrange interpolants.

The errors $|||u_h - u|||_{\varepsilon;\Omega}$ are compared with the corresponding estimators $\mathcal{E}$ in Table 8.1. One observes that the effectivity indices (computed as the ratio of the estimator to the error) do not exceed 1.361.

We also look at two components of the the error in the energy norm. It is reasonable to assume that

$$|||u_h - u|||_{\varepsilon;\Omega} \simeq \left\{\varepsilon^2 \|\nabla u_h - (\nabla u)^I\|_\Omega^2 + \|u_h - u^I\|_\Omega^2\right\}^{1/2} + \|u - u^I\|_\Omega \,. \tag{8.1}$$

This error decomposition is useful as the two error components in (8.1) exhibit somewhat different behaviour in our experiments, as $\simeq \varepsilon^{1/2} N^{-1}$ and $\simeq N^{-2}$, respectively (compare the upper parts of Tables 8.2 and 8.3). Furthermore, one can identify that $\mathcal{E}\big|_{f_h := f_h^I}$ (obtained from (4.2) by replacing f_h with its linear interpolant f_h^I) essentially estimate the first error component in (8.1) (see Table 8.2), while $\|f_h - f_h^I\|_\Omega$ provides a reasonable estimator for the remaining error component in (8.1) (see Table 8.3). Indeed, for the estimator components in Tables 8.2 and 8.3 (for the latter, when $\varepsilon \leqslant 2^{-5}$), the effectivity indices do not exceed 1.374.

For the considered ranges of ε and N, the aspect ratios of the mesh elements take values between 2 and 3.6e+8. Considering these variations, our estimator $\mathcal{E}$ performs quite well and its effictivity indices do not exceed 1.337 and stabilize to 1 as $\varepsilon \to 0$. A more comprehensive numerical study of the proposed estimator certainly needs to be conducted, and will be presented elsewhere.

REFERENCES

[1] M. Ainsworth and I. Babuška, *Reliable and robust a posteriori error estimating for singularly perturbed reaction-diffusion problems*, SIAM J. Numer. Anal., 36 (1999), pp. 331–353.

[2] M. Ainsworth and J. T. Oden, *A posteriori error estimation in finite element analysis*, Wiley-Interscience, New York, 2000.

[3] M. Ainsworth and T. Vejchodský, *Fully computable robust a posteriori error bounds for singularly perturbed reaction-diffusion problems*, Numer. Math., 119 (2011), pp. 219–243.

[4] M. Ainsworth and T. Vejchodský, *Robust error bounds for finite element approximation of reaction-diffusion problems with non-constant reaction coefficient in arbitrary space dimension*, Comput. Methods Appl. Mech. Engrg., 281 (2014), pp. 184–199.

[5] N. S. Bakhvalov, *On the optimization of methods for solving boundary value problems with boundary layers*, Zh. Vychisl. Mat. Mat. Fis., 9 (1969), pp. 841–859 (in Russian).

[6] N. M. Chadha and N. Kopteva, *Maximum norm a posteriori error estimate for a 3d singularly perturbed semilinear reaction-diffusion problem*, Adv. Comput. Math., 35 (2011), pp. 33–55.

[7] I. Cheddadi, R. Fučík, M. I. Prieto and M. Vohralík, *Guaranteed and robust a posteriori error estimates for singularly perturbed reaction diffusion equations*, M2AN Math. Model. Numer. Anal. 43 (2009), pp. 867–888.

[8] C. Clavero, J. L. Gracia and E. O'Riordan, *A parameter robust numerical method for a two dimensional reaction-diffusion problem*, Math. Comp., 74 (2005), pp. 1743–1758.

[9] A. Demlow and N. Kopteva, *Maximum-norm a posteriori error estimates for singularly perturbed elliptic reaction-diffusion problems*, Numer. Math., 133 (2016), pp. 707–742.

[10] S. Grosman, *An equilibrated residual method with a computable error approximation for a singularly perturbed reaction-diffusion problem on anisotropic finite element meshes*, M2AN Math. Model. Numer. Anal., 40 (2006), pp. 239–267.

[11] N. Kopteva *Maximum norm error analysis of a 2d singularly perturbed semilinear reaction-diffusion problem*, Math. Comp., 76 (2007), pp. 631–646.

[12] N. Kopteva, *Maximum norm a posteriori error estimate for a 2d singularly perturbed reaction-diffusion problem*, SIAM J. Numer. Anal., 46 (2008), pp. 1602–1618.

[13] N. Kopteva, *Linear finite elements may be only first-order pointwise accurate on anisotropic triangulations*, Math. Comp., 83 (2014), pp. 2061–2070.

[14] N. Kopteva, *Maximum-norm a posteriori error estimates for singularly perturbed reaction-diffusion problems on anisotropic meshes*, SIAM J. Numer. Anal., 53 (2015), pp. 2519–2544.

[15] N. Kopteva, *Energy-norm a posteriori error estimates for singularly perturbed reaction-diffusion problems on anisotropic meshes*, (2016), submitted for publication, `http://www.staff.ul.ie/natalia/pubs.html`.

[16] N. Kopteva, *Energy-norm a posteriori error estimates for singularly perturbed reaction-diffusion problems on anisotropic meshes. Neumann boundary conditions*, (2016) submitted for publication, `http://www.staff.ul.ie/natalia/pubs.html`.

[17] N. Kopteva and E. O'Riordan, *Shishkin meshes in the numerical solution of singularly perturbed differential equations*, Int. J. Numer. Anal. Model., 7 (2010), pp. 393–415.

[18] G. Kunert, *An a posteriori residual error estimator for the finite element method on anisotropic tetrahedral meshes*, Numer. Math., 86 (2000), pp. 471–490.

[19] G. Kunert, *Robust a posteriori error estimation for a singularly perturbed reaction-diffusion equation on anisotropic tetrahedral meshes*, Adv. Comput. Math., 15 (2001), pp. 237–259.

[20] G. Kunert and R. Verfürth, *Edge residuals dominate a posteriori error estimates for linear finite element methods on anisotropic triangular and tetrahedral meshes*, Numer. Math., 86 (2000), pp. 283–303.

[21] H.-G. Roos, M. Stynes and L. Tobiska, *Robust Numerical Methods for Singularly Perturbed Differential Equations*, Springer, Berlin, 2008.

[22] K. G. Siebert, *An a posteriori error estimator for anisotropic refinement*, Numer. Math., 73 (1996), pp. 373–398.

[23] R. Verfürth, *Robust a posteriori error estimators for a singularly perturbed reaction-diffusion equation*, Numer. Math., 78 (1998), pp. 479–493.